THE PENNSYLVANIA STATE UNIVERSITY
SCHREYER HONORS COLLEGE

DEPARTMENT OF BIOCHEMISTRY AND MOLECULAR BIOLOGY

Adenylosuccinate Lyase Plays a Role in Neuromuscular Coordination

MIA PEIFER
SPRING 2024

A thesis
submitted in partial fulfillment
of the requirements
for a baccalaureate degree
in Biochemistry and Molecular Biology
with honors in Biochemistry and Molecular Biology

Reviewed and approved* by the following:

Wendy Hanna-Rose
Professor of Biochemistry and Molecular Biology
Thesis Supervisor

Timothy C. Meredith
Associate Professor of Biochemistry and Molecular Biology
Honors Adviser

* Electronic approvals are on file.

ABSTRACT

Adenylosuccinate Lyase (ADSL) Deficiency is an ultra-rare purine metabolic disorder that results in severe neurobehavioral and neuromuscular defects. My lab has established an *adsl-1* deficient *Caenorhabditis elegans* (*C. elegans*) model with phenotypes of altered learning, loss of muscle mass and integrity, and locomotive defects. Locomotive defects include slowed mobility and a distinct lack of coordination revealed by the inability to regulate the size of the body bend angles during swimming movement. Among the locomotive defects associated with an *adsl-1* deficiency, we are particularly interested in understanding the mechanisms that cause *adsl-1* animals to lose the ability to regulate body bending.

Our *adsl-1* deficient model has been useful in studying the mechanisms that underlie learning and neuromuscular defects associated with ADSL Deficiency. Because patients with ADSL Deficiency suffer from severe neuromuscular defects, I am interested in understanding the neural mechanisms that control the muscle function necessary to regulate body bending during swimming movement. I hypothesized that the inability to regulate body bending exhibited by *adsl-1* deficient animals could be a result of perturbations to neural regulation of muscle function. To test this hypothesis, I reasoned that it would be optimal to first explore how the existing phenotypes associated with the loss of *adsl-1* function contribute to coordination. This approach allowed me to determine whether any other pleiotropic effects of an *adsl-1* deficiency contribute to the animal's inability to regulate body bending before investigating the nervous system of *C. elegans*, which is its most complex system.

To determine if these pleiotropic phenotypes play a role in neuromuscular coordination, I genetically and pharmacologically manipulated normal and *adsl-1* deficient *C. elegans* and investigated how perturbations to tyramine signaling, muscular structural defects, general unhealthiness, and an inability to maintain normal rates of locomotion influence coordination.

I found that *adsl-1* animals share phenotypes with animals that have perturbations to tyramine signaling. This evidence supports the hypothesis that tyramine production is reduced upon the loss of

adsl-1 function. However, further analysis of *adsl-1* deficient animals and tyramine deficient animals suggests that reduced tyramine production does not play a role in the locomotive phenotypes associated with the loss of *adsl-1* function.

Thus, I explored alternative hypotheses for what contributes to the locomotive phenotypes associated with the loss of *adsl-1* function with particular emphasis on understanding the etiology of the *adsl-1*-related coordination phenotype. I hypothesized that muscle weakness, slowed development, or reduced energy metabolism associated with an *adsl-1* deficiency is causative of the coordination phenotype. I found that while these characteristics alone resulted in slowed mobility, they were not sufficient to recreate the coordination phenotype. As slowed mobility did not cause a lack of coordination, I sought to determine if the inability to maintain normal rates of swimming locomotion could directly cause animals to lose the ability to coordinate body bending during swimming. I observed swimming movement of animals with hyperactive muscle contraction and found evidence that suggests an animal's inability to maintain normal rates of swimming locomotion does not directly impact coordination.

My research suggests that perturbations to tyrosine metabolism, muscle structural defects, general unhealthiness, or the inability to maintain normal rates of locomotion associated with an *adsl-1* deficiency do not directly cause the lack of coordination *adsl-1* animals bend angle distribution reveals. These findings suggest that neural function of *adsl-1* could play a key role in maintaining coordination. If so, the coordination phenotype could be useful for studying the role of *adsl-1* in the neuron by serving as a model of the complex neurological and neuromuscular symptoms of an ADSL Deficiency. Understanding the mechanisms of the coordination phenotype and the role of *adsl-1* in the neuron could be useful in providing new potential targets for the development of novel therapeutics that can be used to treat the devastating neuromuscular symptoms associated with ADSL Deficiency.

TABLE OF CONTENTS

LIST OF FIGURES

LIST OF TABLES

LIST OF ABBREVIATIONS

PRPP	phosphoribosyl diphosphate
PRA	ribosylamine-5-phosphate
GART	phosphoribosylglycinamide formyltransferase
PAICS	phosphoribosylaminoimidazole succinocarboxamide synthetase
AIR	aminoimidazole ribotide
CAIR	carboxyaminoimidazole ribonucleotide
ADSL	adenylosuccinate lyase
SAICAR	succinyl aminoimidazole carboxamide ribotide
AICAR	aminoimidazole carboxamide ribotide
N^{10}-Formyl THF	N^{10}-formyltetrahydrofolate
IMP	inosine monophosphate
S-AMP	succinyladenosine monophosphate
AMP	adenosine monophosphate
GMP	guanosine monophosphate
ARPT	adenine phosphoribosyl transferase
HGPRT	hypoxanthine-guanine phosphoribosyl transferase
S-Ado	succinyladenosine
SAICAr	succinylaminoimidazole carboxamide riboside
LMX	lometrexol
MTX	methotrexate
NA	nicotinic acid
NAD^+	nicotinamide
LNS	Lesch Nyhan Syndrome

UDGP	uridine diphosphate glucose
RNAi	RNA interference

ACKNOWLEDGEMENTS

Thank you to Dr. Wendy Hanna-Rose. Her mentorship and support throughout this thesis project and during my entire undergraduate research experience have been invaluable to my development as a scientist. Thank you to Dr. Latisha Franklin for guiding me personally and professionally through the challenges I have faced as an undergraduate student. Thank you to Kareem who has always been willing to answer my questions and Dr. Sampurna Sattar who taught me how to pick a worm. I would also like to thank Rishika, Maia, Sabrina, Juan, and all the other members of the Hanna-Rose Lab for being amazing lab mates and friends and for supporting me throughout these past two years. Finally, thank you to my family for their continued love and support throughout my undergraduate studies.

I would like to acknowledge the BMB Scholars Program, the Eberly College of Science, the Society for Industrial Biotechnology, and a J. Loyd Huck Biotechnology Mini-grant from the Huck Institute of Life Science for supporting this research. This work was also supported by NIH NINDS Award #R03NS096451 to WHR. The funders had no role in study design, data collection and analysis, decision to publish, or preparation of the manuscript. Any opinions, findings, conclusions, or recommendations expressed in this thesis are those of the authors(s) and do not necessarily reflect the views of the funders.

Chapter 1

Introduction

Inborn errors of purine and pyrimidine metabolism are rare genetic disorders associated with perturbations to the pathways that synthesize and recycle purine and pyrimidine nucleotides. These disorders are inherited and are a result of changes in enzymatic activity due to mutations in the genes that encode key enzymes involved in purine and pyrimidine biosynthesis and salvage. Currently, there are 17 inborn errors of purine and pyrimidine metabolism that cause disease in humans, and they are typically diagnosed using metabolite screening and genetic testing[1,2].

Our lab is interested in understanding inborn errors in purine metabolism and searching for new ways to treat their devastating symptoms. For many of these disorders, alterations to enzymatic activity are reflected by the accumulation of purine pathway intermediate substrates and the absence of purine products in the urine, blood, or cerebrospinal fluid[3]. Changes in the concentration of purine metabolites are associated with the development of neurological, nephrological, and muscular defects[1]. However, the mechanisms that underlie the development of these symptoms are poorly understood. Despite our awareness of inborn errors of purine metabolism and our ability to test for them, they are infrequently diagnosed due to the variability of their symptoms[1].

In 1999, a survey of 18 European countries, with a population exceeding 435 million, revealed just 835 existing diagnoses, most of which were reported in regions with the appropriate technology necessary for diagnosis[4]. This lack of prevalence, in conjunction with proper diagnoses at institutions equipped with sufficient technology, suggests that these numbers do not reflect the true population of individuals affected by these disorders.

Purine metabolic disorders are not only underdiagnosed but sometimes misdiagnosed as other neurological disorders. One example was in 1984 when a 10-year-old boy, previously diagnosed with

cerebral palsy, began showing symptoms of Lesch-Nyhan Syndrome, an inborn error of purine metabolism associated with perturbations to purine salvage. It was only after these symptoms had become apparent that he was tested for Lesch-Nyhan Syndrome and properly rediagnosed[5].

Due to their rarity, purine metabolic disorders are understudied, and few strategies have been developed to treat them. Many of the mechanisms underlying the development of their devastating symptoms are poorly understood. Understanding these mechanisms is of major clinical significance as they could provide some of the most effective therapeutic targets. It is imperative that we understand how these symptoms arise so we can bring greater awareness to inborn errors of purine metabolism and provide solutions and support for those who suffer from them.

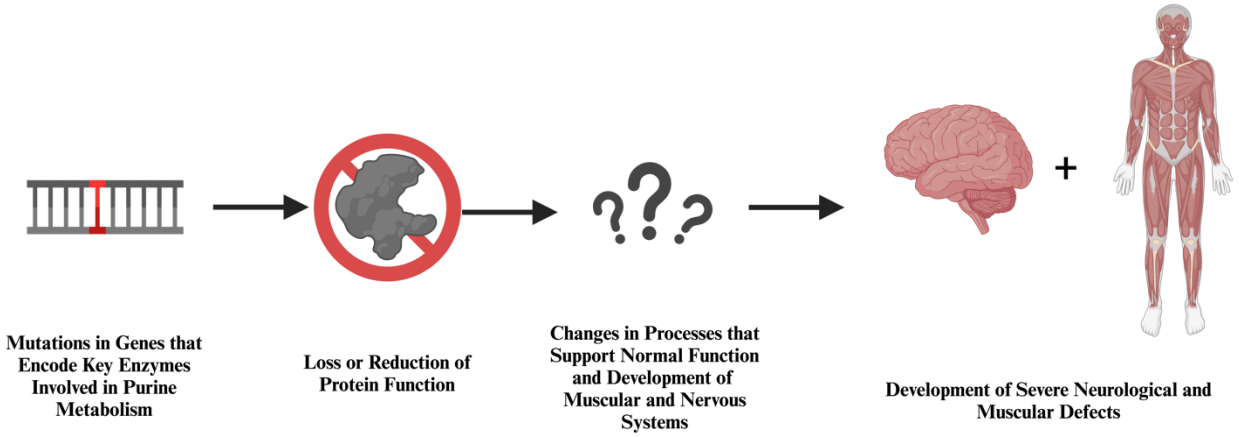

Figure 1. Mutations in genes encoding enzymes in purine metabolism cause nervous and muscular symptoms to be affected. The mechanisms that exists between between enzyme function and symptoms development remain unknown.

Overview of Purine Metabolism

The purine products adenine, adenosine monophosphate (AMP), guanine, and guanosine monophosphate (GMP) play an important role in many vital biological processes. They are synthesized through either *de novo* synthesis or the salvage cycle (Figure 2). Under normal conditions, purine nucleotides, which are required for many biological processes, are generated by recycling purine bases through the less energy expensive salvage cycle[6]. Under conditions where purines are in high demand, *de novo* synthesis is upregulated.

de novo purine biosynthesis is a 10-step process that generates purines through the energy and resource-expensive formation of the pyrimidine and imidazole rings (Figure 2). Conversion of phosphoribosyl diphosphate (PRPP) from the pentose phosphate pathway to ribosylamine-5-phosphate (PRA) initiates and commits the cell to using that sugar-phosphate for *de novo* purine synthesis. Three of the first four steps are catalyzed by phosphoribosylglycinamide formyltransferase (GART), which requires the coenzyme N^{10}-formyltetrahydrofolate (N^{10}-Formyl THF) that is generated through one-carbon metabolism.

Following the third GART reaction, phosphoribosylaminoimidazole succinocarboxamide synthetase (PAICS) acts twice to convert aminoimidazole ribotide (AIR) to carboxyaminoimidazole ribonucleotide (CAIR) and CAIR to succinyl aminoimidazole carboxamide ribotide (SAICAR). SAICAR is then converted by adenylosuccinate lyase (ADSL) to aminoimidazole carboxamide ribotide (AICAR) leaving fumarate as a byproduct.

The final step of *de novo* synthesis produces inosine monophosphate (IMP) which is ultimately converted to AMP or GMP. Subsequently, AMP and GMP are converted to adenine and guanine. Adenine and guanine are recycled back to AMP and GMP by the salvage enzymes adenine phosphoribosyl transferase (APRT) and hypoxanthine-guanine phosphoribosyl transferase (HGPRT).

Products of purine nucleotide biosynthesis and salvage can be used by the body to synthesize DNA and RNA, provide cellular energy, and provide intracellular signals[6]. They can also be further broken down by the cell and excreted in the form of uric acid.

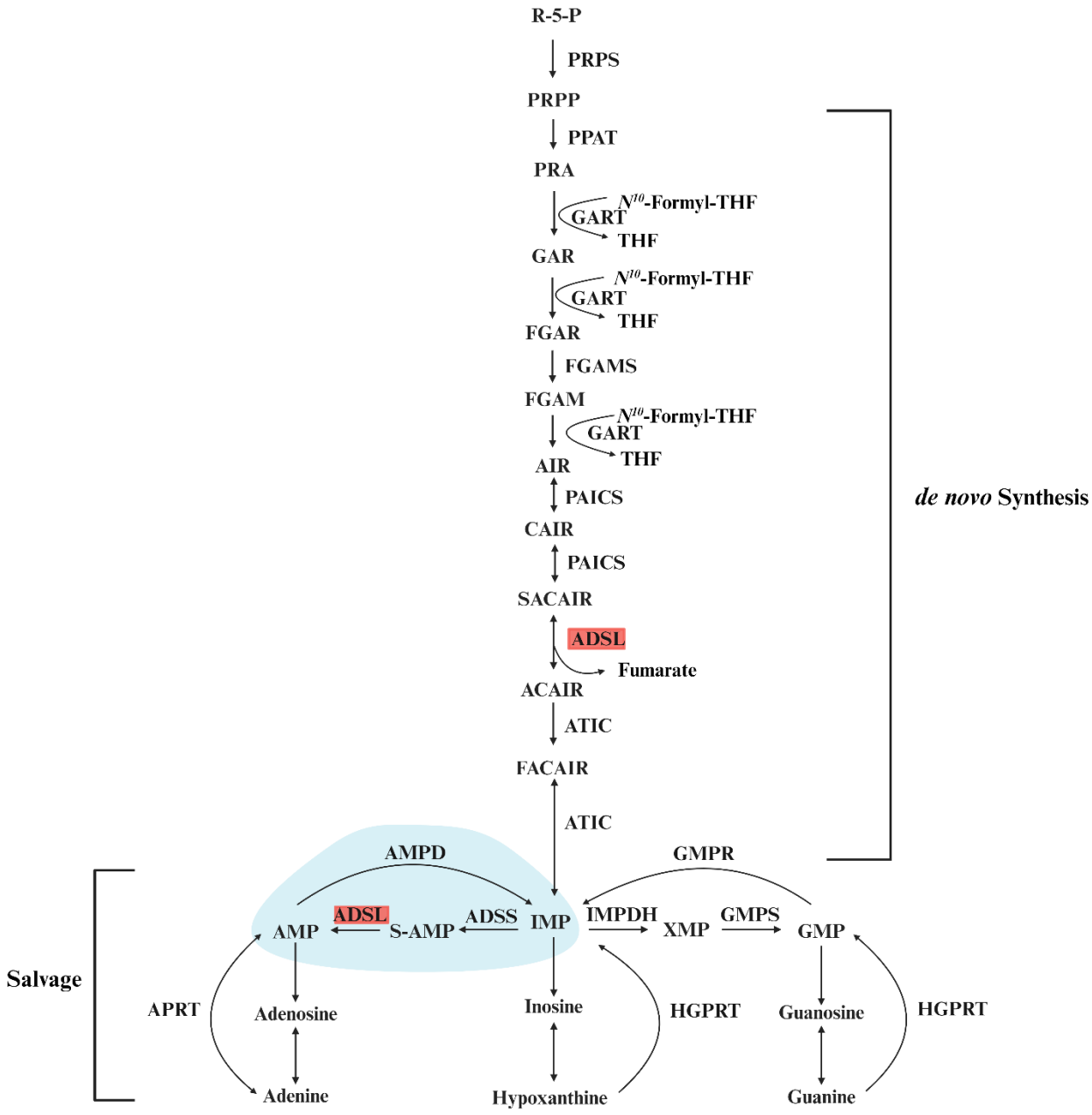

Figure 2. Purine metabolism pathway. Purines are generated through *de novo* synthesis and the salvage cycle. Adenylosuccinate lyase (ADSL), which is involved in *de novo* synthesis and, later, in the purine nucleotide cycle, is highlighted in red. The purine nucleotide cycle is highlighted in blue.

Adenylosuccinate Lyase Deficiency

Adenylosuccinate Lyase (ADSL) catalyzes two reactions in purine biosynthesis. During *de novo* synthesis, ADSL converts SAICAR to AICAR. Within the purine nucleotide cycle (Table 2), ADSL converts succinyladenosine monophosphate (S-AMP) to adenosine monophosphate (AMP). ADSL's role in the PNC is important in maintaining fumarate levels and ATP/AMP ratios in the muscles[7].

ADSL Deficiency is an autosomal recessive disorder caused by a variety of mutations in the ADSL gene[8]. It was first identified in 1984 when Jaeken and Van den Berghe noticed an accumulation of the succinyl purines succinyladenosine (S-Ado) and SAICA-riboside (SAICAr) in the cerebrospinal fluid, plasma, and urine of three patients who presented with symptoms of autistic-like behavior, psychomotor defects, ataxia, hypotonia, and failure to make eye contact. Upon further study of these individuals, they discovered a significant reduction of ADSL activity in the liver and a complete loss of its function in the kidney[9].

The most severe form of ADSL Deficiency, the neonatal form, is associated with intractable seizures and respiratory failure that leads to early fatality[10,11]. The other two forms of ADSL Deficiency, Type I and Type II, are usually diagnosed in the first few years of life. The Type I form is the most common. It is more severe than Type II and is characterized by uncontrollable seizures, psychomotor delay, autistic-like features, and persistent failure to make eye contact. Patients with Type II ADSL Deficiency have mild to moderate psychomotor delay, disturbances in eye contact, and are sometimes nonverbal. Both forms can cause dysmorphic features including microcephaly, flat occiput, small, upturned nose, low set ears, and thin upper lips[9–12]. Currently, there is no well-defined threshold between Type I and Type II characteristics.

Testing for ADSL Deficiency is typically performed as symptoms arise during early life by screening the urine, cerebrospinal fluid, or erythrocytes. Currently, there are no existing strategies specific to treating ADSL Deficiency, and, because it is understudied, there is a lack of therapeutic development.

Of the treatments that have been tested, administration of D-ribose, to stimulate *de novo* synthesis by increasing the amount of PRPP available to the cell, was reported to progressively reduce seizures and slightly improve behavior[13]. Others exploring D-ribose treatment have found no positive effect[14]. Uridine supplementation reduced the number of seizures a 15-year-old patient with ADSL Deficiency experienced and decreased levels of uric acid in their blood and urine[13,15].

A few hypotheses have been proposed to explain the severity of ADSL Deficiency's symptoms. Lower ratios of S-Ado to SAICAr in the cerebrospinal fluid have been attributed to more severe symptoms suggesting that SAICAr is toxic[11,16]. Evidence supporting SAICAr toxicity has been described using *C. elegans*, human epithelial cells, and zebrafish embryos[17,18]. However, a detailed mechanism of SAICAr toxicity and its interactome has yet to be discovered. Others have hypothesized that a deficiency of purines during embryonic development could cause ADSL Deficiency's wide range of neurological defects[19] or that loss of ADSL function can cause the disorder through perturbations to the PNC[7].

Due to its clinical significance, ADSL Deficiency has been modeled in several systems including *C. elegans*, chicken embryos, zebrafish, and human epithelial cells[17,18,20]. Adenylosuccinate lyase deficient models have been useful for studying the metabolic, developmental, learning, and neuromuscular symptoms associated with ADSL Deficiency. ADSL-related neurobehavioral and neuromuscular symptoms are arguably the most important aspects of the disorder that we should be addressing as they are the most prevalent, complex, and life-threatening symptoms. Our lab has characterized several neurobehavioral and neuromuscular phenotypes associated with an *adsl-1* deficiency in *C. elegans* [18,21,22], but our understanding of the mechanisms that dictate their development and severity is still limited.

Modeling Adenylosuccinate Lyase Deficiency in *C. elegans*

Through RNAi knockdown or deletion of *adsl-1,* the *Caenorhabditis elegans* (*C. elegans*) homolog for ADSL, our lab, and others, have been able to model ADSL Deficiency. Loss of *adsl-1* via RNAi knockdown results in severe perturbations to gonad morphology, reduced brood size, and an increase in embryonic lethality[21]. The *adsl-1(tm3328)* mutant strain, with a large deletion in the *adsl-1* gene, results in failed gonad development which causes sterility, significantly slowed development, reduction of body size, loss of muscle integrity, and mobility defects [21,23].

Loss of muscle integrity due to an *adsl-1* deficiency leads to disorganized muscle myosin and reduced muscle mass[23]. Disorganized muscle myosin and reduced muscle mass are likely linked to some of the locomotive phenotypes associated with the loss of *adsl-1* function but are not responsible for the full breadth of them. Mobility or locomotive defects associated with an *adsl-1* deficiency include slowed swimming (Figure 3B) and thrashing (Figure 3A) and an increase in spontaneous reversals. They also display a distinct inability to regulate the angles at which they bend their bodies as revealed by complete randomization of body bend angles during swimming movement (Figure 3D) [21,22]. An interesting characteristic of this coordination phenotype is that the mean maximum bending angle of *adsl-1* animals is indistinguishable from the N2 control (Figure 3C). This, along with the animal's ability to generate large bends, suggests that *adsl-1* mutants are not weak[22].

In addition to these phenotypes, an *adsl-1* deficiency changes metabolism. Like in humans, an *adsl-1* deficiency causes SAICAr and S-Ado to accumulate and fumarate to become reduced. Evidence supporting the contribution of SAICAr toxicity to reversal phenotypes and mobility defects was found through treatment of *adsl-1(tm3328)* and *adsl-1* RNAi animals with the GART inhibitor lometrexol (LMX), and the antifolate, methotrexate (MTX)[21]. Supplementation of purines has restorative effects on fertility[21]. Further metabolomic analysis revealed that lack of *adsl-1* function led to the accumulation of tyrosine[18].

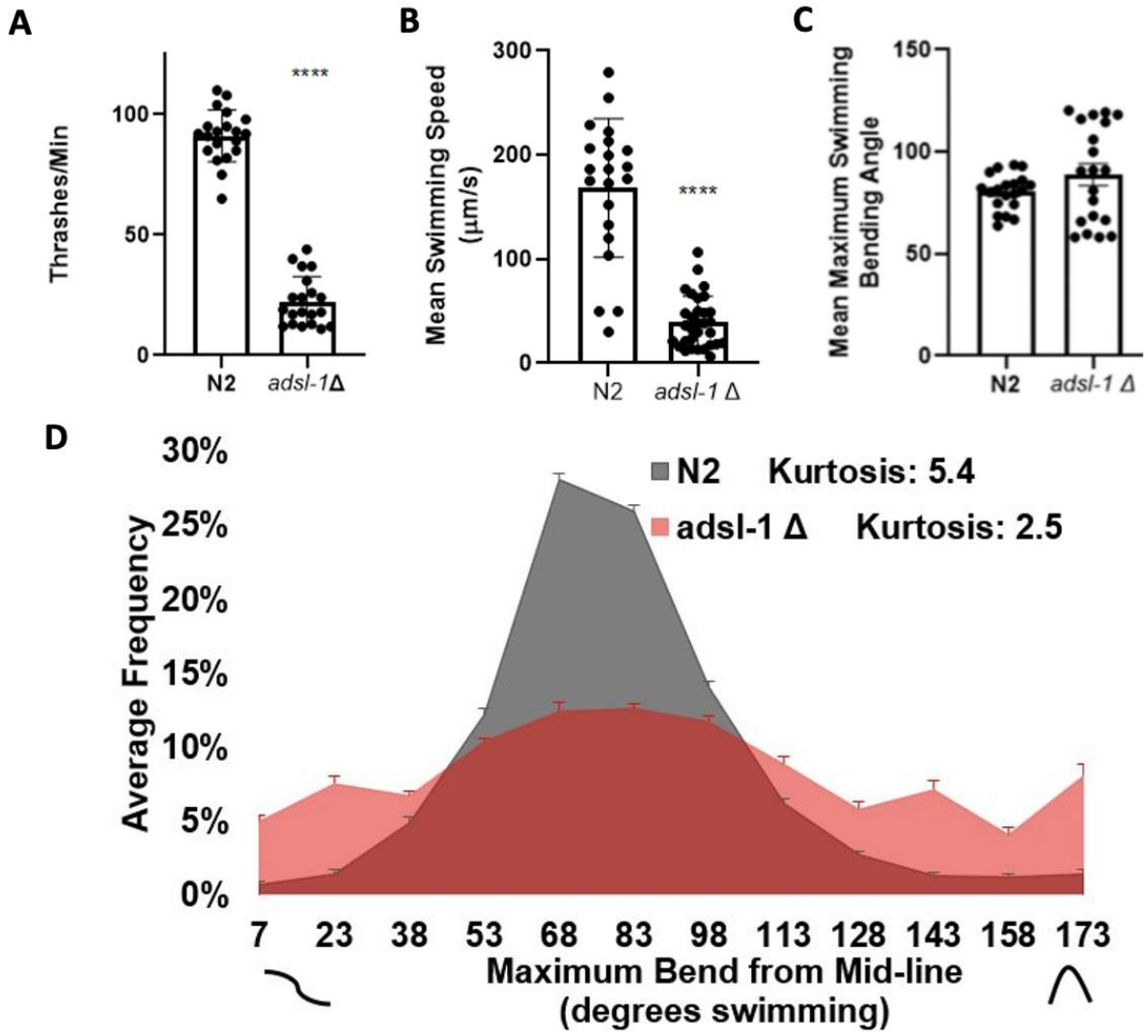

Figure 3. Locomotive phenotypes associated with the loss of *adsl-1* function. *adsl-1* animals have (A) slowed thrashing rates, (B) slower swimming speeds, (C) no change in mean maximum bending angle, and (D) do not prefer to swim with a specific range of body bend angles. In panels A, B, and C, each circle represents a value for a single animal. A student's unpaired t test was used to determine significance. **** represents $p<0.0001$. Maximum bending angles during swimming movement were plotted as a frequency distribution in panel D. Panels A, C, and D were derived from the same 20 animals. Panel B was derived from a second set of animals (N2 n=21 and *adsl-1* n=32). * Figure adapted from Franklin, Patil, Peifer, Fenton, Hartmann, Hanna-Rose submitted August 2023.

Tyrosine Metabolism in *C. elegans*

Tyrosine is an amino acid and serves as a precursor of three important biogenic amines: tyramine, octopamine, and dopamine. Tyrosine can be converted to tyramine by tyrosine decarboxylase (*tdc-1*) or to L-Dopa by tyrosine 3-monooxygenase (*cat-2*). Tyramine acts as a neurotransmitter in *C. elegans* to regulate egg-laying activity, reversal behavior, and suppression of head oscillations while backing[24]. *C. elegans* with loss of *tdc-1* activity have altered learning[18,24].

Dopamine also acts as a neurotransmitter in *C. elegans.* It plays a major role in locomotion. For example, after extended periods of swimming, dopamine accumulates in the synapse, and, if not shuttled out of the synapse quickly enough, leads to paralysis through extrasynaptic activity[25]. It also plays a key role in transitioning from the crawling to swimming gait and aids in maintaining swimming movements following bouts of crawling[26]. During crawling, dopamine has also been shown to act as a regulator of locomotive rates[27] and contributes to food-dependent basal slowing behavior[28].

C. elegans Locomotion

Similar to snakes and fish, nematodes use dorsoventral undulatory motion to propel themselves on surfaces and through liquid environments[29]. This motion is produced through the interplay of the nervous and muscular systems which work together to sense the animal's environment, send signals through the neuromuscular junction, generate the force required for muscle contraction, and coordinate contraction and relaxation of the body wall muscles[29,30].

Undulatory motion has been connected to the velocity, or speed, of the animals with a higher frequency of undulations correlating with higher speeds[31]. The frequency of undulation, in liquid environments, is described by thrashing rate. During thrashing movements, *C. elegans* bend their bodies side to side producing a "C" shape at the top of each thrash. Smaller body bends while thrashing suggest animals have muscle weakness[30]. Large body bends can be described by curling events. Curling is characterized by the "O" or "6" shapes an animal produces while thrashing. Muscle weakness and curling events are known to contribute to changes in swimming behavior, but *C. elegans* locomotion is complex and these characteristics are likely just a fraction of the ways we can begin to describe swimming phenotypes. An example of this complexity and our lack of understanding of how characteristics like muscle weakness or curling behavior impact normal swimming locomotion becomes evident through observation of *adsl-1* mutants' coordination. *adsl-1* mutants lack the ability to regulate swimming bending angle. However, they do not seem to be weak as mean maximum bending angle is not smaller than the control (Figure 3)[22].

Locomotion can be easily analyzed and quantified by manual observation or by recording and tracking movement through a computer software. Changes in locomotion, for example, increased reversing or rolling, can provide insight into development and neural or muscular function. Identifying locomotive phenotypes has played an invaluable role in developing models to study disease and the effects of various treatments.

Overview

As there are limited models that are efficient for studying the neurobehavioral and neuromuscular symptoms associated with ADSL Deficiency, our lab aims to contribute to the development of these models by understanding the mechanisms that underlie phenotypes associated with the loss of *adsl-1* function. Through my research, I aim to expand our understanding of the mechanisms that underlie the locomotive phenotypes, especially the coordination phenotype, associated with the loss of *adsl-1* function in *C. elegans*. ADSL Deficiency can be modeled using either RNAi or mutants with a deletion in the *adsl-1* gene. Throughout this work, I explore phenotypes associated with the *adsl-1* strain with the null, *tm3328,* allele.

In Chapter 2 of this thesis, I explore tyrosine metabolism of *adsl-1* mutants. Through this work, I found that *adsl-1* animals share a head oscillation phenotype with animals that have perturbations to tyramine signaling. Our lab also discovered that *adsl-1* animals have altered learning phenotypes that are tyramine dependent. Head oscillation and altered learning phenotypes can be used to model some of the neurological symptoms associated with ADSL Deficiency. Next, I explore the effects of *adsl-1*-related perturbations to tyrosine metabolism on locomotive phenotypes. I found that tyramine signaling, and more broadly tyrosine metabolism, had no impact on locomotion and that defects in tyramine signaling do not explain the mechanisms underlying ADSL Deficiency's neuromuscular symptoms.

In Chapter 3 of this thesis, I explore the factors that contribute to the locomotive phenotypes associated with *adsl-1* with particular emphasis on the coordination phenotype. I hypothesized that muscle weakness or the pleiotropic effects of an *adsl-1* deficiency that impact energy metabolism cause the animals to lose their ability to regulate the angles at which they bend their bodies during swimming movement. I found that while muscle weakness or perturbations to energy alone caused slowed mobility, they were not sufficient to recreate the coordination phenotype. My research suggests that defects in tyrosine metabolism, muscular structure and function, energy metabolism, or the maintenance of normal

rates of swimming locomotion are not sufficient to cause *C. elegans* to lose the ability to regulate the angles at which they bend their bodies during swimming movement.

I then hypothesized that an animal's ability to maintain normal rates of locomotion may directly cause the coordination phenotype but found that this was not the case. These findings together suggest that a more complex mechanism exists to maintain coordination and that possibly neural function of *adsl-1* is involved. If so, the coordination phenotype could be useful for studying the role of *adsl-1* in the neuron by serving as a model of the complex neurological and neuromuscular symptoms of an ADSL Deficiency. Further, understanding the mechanisms of this phenotype may provide potential targets for the development of novel therapeutics.

Chapter 2

adsl-1 Deficient Mutants Share Phenotypes with Tyramine Deficient Mutants

*The following data is published: Moro, C. A. *et al.* Adenylosuccinate lyase deficiency affects neurobehavior via perturbations to tyramine signaling in Caenorhabditis elegans. *PLoS Genet* **19**, e1010974 (2023).

Tyrosine accumulates when *adsl-1* function in *C. elegans* is reduced. We hypothesized that accumulation of tyrosine may be a result of reduced or impaired production of the biogenic amines tyramine and dopamine. We found that the tyrosine decarboxylase mutant, *tdc-1(n3419)*, with a deletion in the *tdc-1* gene and loss of *tdc-1* function phenocopied learning behaviors of *adsl-1(tm3328)* mutants[18]. This led to the hypothesis that *adsl-1* mutants would share other phenotypes with *tdc-1* mutants.

Animals with perturbations to tyramine signaling through loss of *tdc-1* function or ablation of the RIM neurons fail to suppress oscillatory motion during backing[24]. To determine if *adsl-1* mutants share phenotypes with tyramine deficient mutants, I compared head oscillation behavior of *adsl-1* and *tdc-1* mutants during backing induced by gentle touch.

Upon gentle touch, N2 animals suppressed head oscillations during 94% of induced reversals. As expected, *tdc-1* animals lacked the ability to suppress head oscillations with only 9% suppression during induced reversals. *adsl-1* animals suppressed head oscillations during 18% of induced reversals (Figure 4). Reduction in percent suppression when compared to N2 reflects the inability to suppress head oscillations during spontaneous reversals. *adsl-1* animals phenocopied *tdc-1* animals suggesting that tyramine signaling may be perturbed. Further investigation of tyramine signaling in *adsl-1* deficient animals revealed that tyramine supplementation rescues head oscillation phenotypes of *tdc-1* and *adsl-1* animals[18]. These results support the conclusion that tyramine is reduced upon the loss of *adsl-1* function.

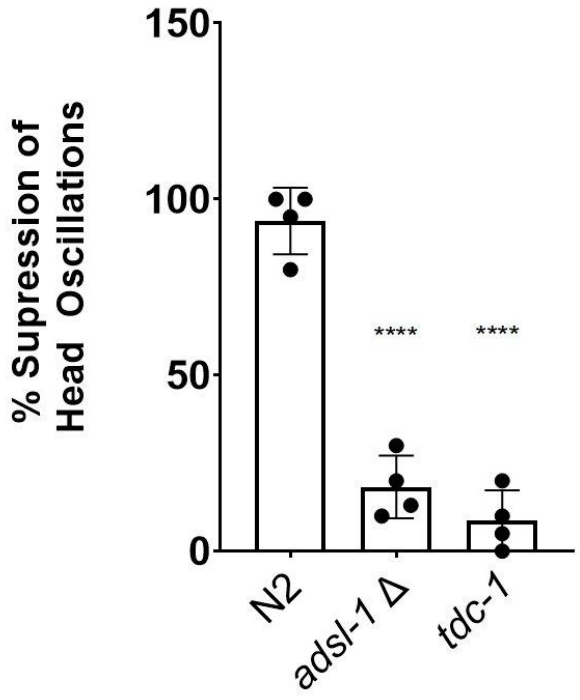

Figure 4. Loss of *adsl-1* function results in failure to suppress head oscillation during spontaneous reversal movement. A gentle touch assay was performed, and percent suppression of head oscillation was compared between N2 control (n=50) and *tdc-1(n3419)* (n=50) and *adsl-1(tm3328)* (n=53) mutant strains. Each dot represents percent suppression of one replicate. An ordinary one-way ANOVA with multiple comparisons was used to determine significance between N2 and *adsl-1* and N2 and *tdc-1* percent suppression. **** corresponds to $p < 0.0001$.

Defects in Tyramine Signaling are not Linked to Movement Phenotypes

Results supporting the conclusion that tyramine is reduced upon the loss of *adsl*-1 function and my interest in understanding the coordination phenotypes of *adsl-1* animals motivated me to explore the role of tyramine in movement. I hypothesized that perturbations to tyramine signaling may influence other locomotive phenotypes displayed by *adsl-1* animals. Because tyramine acts as a neurotransmitter in *C. elegans*[24], I thought this signaling defect may particularly play a role in *adsl-1* animals' inability to coordinate the angles at which they bend their bodies during swimming movement.

To determine if perturbations to tyramine signaling had any effect on locomotion, I observed the swimming behavior of *tdc-1* animals following the same methods as described by Franklin L. P. *et al.* 2023. *tdc-1* animals swam and thrashed faster than the N2 control (Figure 5B, Figure 5A) but did not have any notable differences in the distribution of maximum body bend angles (Figure 5C). Although loss of *tdc-1* function resulted in an increase in swimming speed and thrashing rate, these phenotypes do not reflect the swimming phenotypes associated with the loss of *adsl-1* function. These results suggest that perturbations to tyramine signaling do not contribute to the locomotive phenotypes associated with an *adsl*-1 deficiency.

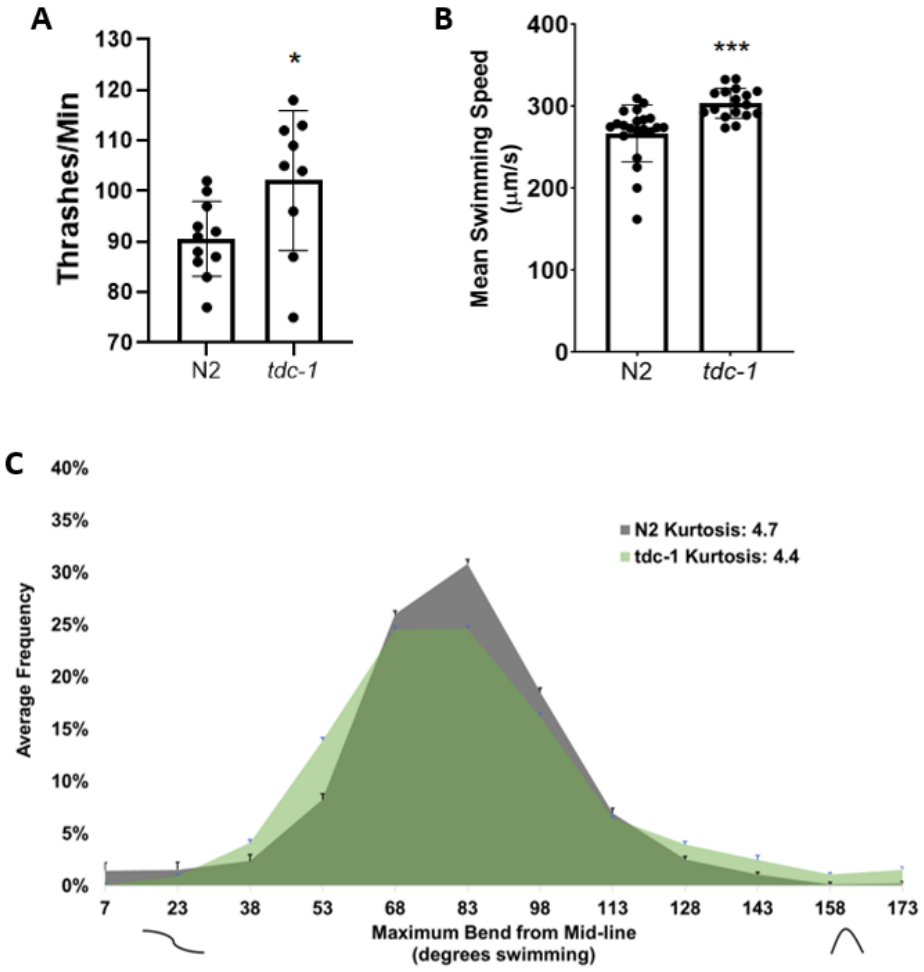

Figure 5. *tdc-1* mutants do not phenocopy *adsl-1*-related locomotive phenotypes. Thrashing (A), swimming speeds (B), and maximum bending angle distribution (C) of *tdc-1(n3419)* mutants do not support the role of tyramine signaling in swimming movement. In panels A and B, each dot represents one animal and a student's t test was used to determine significance. * corresponds to $p<0.05$ and *** corresponds to $p<0.001$. In panels B and C, measurements are taken from the same 20 N2 and 17 *tdc-1* animals. Measurements in panel A are derived from animals assayed in B and C.

Moro *et al.* 2023 found that supplementation of tyramine to both *tdc-1* and *adsl-1* animals rescued the head oscillation phenotype. I hypothesized that, like its effect on neurobehavior, tyramine supplementation may also rescue locomotive phenotypes. To test the effect of tyramine signaling on locomotion, I supplemented *adsl-1* mutants with tyramine hydrochloride (10 mM) and compared their

movement to unsupplemented *adsl-1* mutant animals. Exogenous tyramine slightly decreased swimming speeds (Figure 6B) but had no effect on thrashing rate (Figure 6A) or the distribution of maximum body bend angles (Figure 6C). These results suggest that exogenous tyramine cannot rescue the locomotive phenotypes of *adsl-1* mutants. Further, these results are consistent with the hypothesis that perturbations to tyramine signaling do not contribute to the locomotive phenotypes associated with an *adsl-1* deficiency. I conclude that *adsl-1*-related perturbations to tyramine signaling, as described in the previous section and by Moro *et al.* 2023, are not connected to the *adsl-1*-related locomotive defects observed during swimming movement.

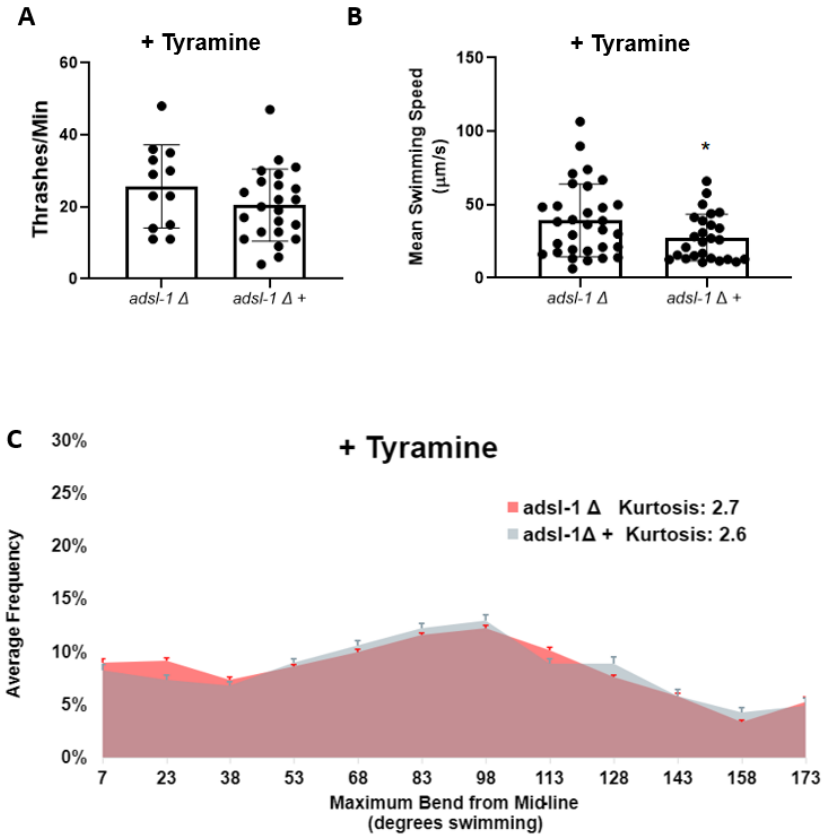

Figure 6. Supplementation of tyramine does not rescue *adsl-1* related locomotive phenotypes. Thrashing (A), swimming speeds (B), and maximum bending angle distribution (C) *adsl-1(tm3328)* mutants supplemented with 10mM tyramine hydrochloride do not support the role of tyramine signaling in swimming movement. In panels A and B, each dot represents one animal and a student's t test was used to determine significance. * corresponds to $p<0.05$. In panel C, *adsl-1*Δ n = 73 and *adsl-1*Δ+ n=28. Measurements in panel B are from 31 of the *adsl-1*Δ animals and the same 28 *adsl-1*Δ+ animals in panel C. Measurements in panel A are derived from animals assayed in panel B.

I alternatively hypothesized that tyramine deficiencies may reflect general alterations to tyrosine metabolism, which could affect dopamine signaling and contribute to the coordination phenotypes observed in *adsl-1* deficient animals. To determine if perturbations to dopamine signaling impact swimming locomotion, I analyzed the swimming behavior of *cat-2(e1112)* mutants, which are dopamine deficient, and *adsl-1* mutants supplemented with various concentrations of dopamine.

cat-2 animals thrashed (Figure 7A) and swam (Figure 7B) significantly faster than the N2 lab control strain. Further, a loss of *cat-2* activity had no major effects on the distribution of maximum bend angle (Figure 7C). These results suggest that loss of *cat-2* function plays a role in maintaining swimming speeds and thrashing rates generally. However, it likely does not contribute to the slowed swimming and thrashing, or the lack of coordination associated with the loss of *adsl-1* activity.

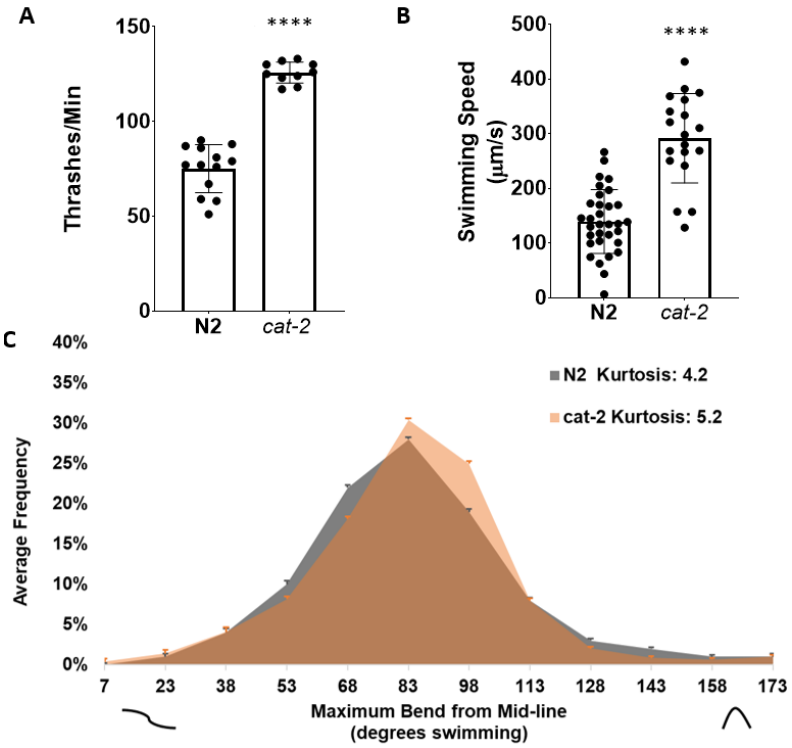

Figure 7. Loss of *cat-2* activity does not induce *adsl-1* related locomotive phenotypes. Thrashing rate (A), swimming speed (B), and distribution of maximum bending angle (C) during swimming movement of *cat-2(e1112)* animals is compared to that of N2. Measurements in panels B and C are from the same 32 N2 and 19 *cat-2* animals. Measurements in panel A are derived from animals assayed in panels B and C. In panels A and B, each dot represents one animal and a student's t test was used to determine significance. **** represents $p<0.0001$.

To further assess the link between tyrosine metabolism and an *adsl-1* deficiency, I analyzed the swimming behavior of *adsl-1* mutants supplemented with various concentrations of dopamine to see if locomotive phenotypes could be restored. Supplementation of 4 mM dopamine slightly reduced N2 animals swimming speeds (Figure 7B), but this reduction in mean swimming speeds may be due to the small fraction of unsupplemented and 8 mM supplemented N2 animals that swim with abnormally fast speeds. Why this small fraction of animals moves more quickly is unclear. Despite minor changes in N2 swimming speeds upon dopamine supplementation, swimming speeds (Figure 8B) and thrashing rates (Figure 8A) of *adsl-1* animals did not improve. Higher concentrations of dopamine caused the distribution of bending angles to shift left (Figure 8C). This left shifting suggests that smaller body bends occur more frequently with higher concentrations of dopamine. Additionally, any concentration of dopamine caused the number of small body bend angles to be greater than both the N2 (Figure 8C, Figure 8D) and *adsl-1* control.

Although dopamine supplementation had some effect on mobility, maximum bending angle distributions of supplemented *adsl-1* animals are not rescued and do not reflect the distributions of N2 animals. Swimming and thrashing rates were also not rescued. These results paired with the locomotion of *cat-2* mutants suggest that dopamine production or dopamine signaling does not play a role in the locomotive phenotypes associated with an *adsl-1* deficiency. I conclude that general perturbations to tyrosine metabolism do not induce the swimming phenotypes associated with an *adsl-1* deficiency.

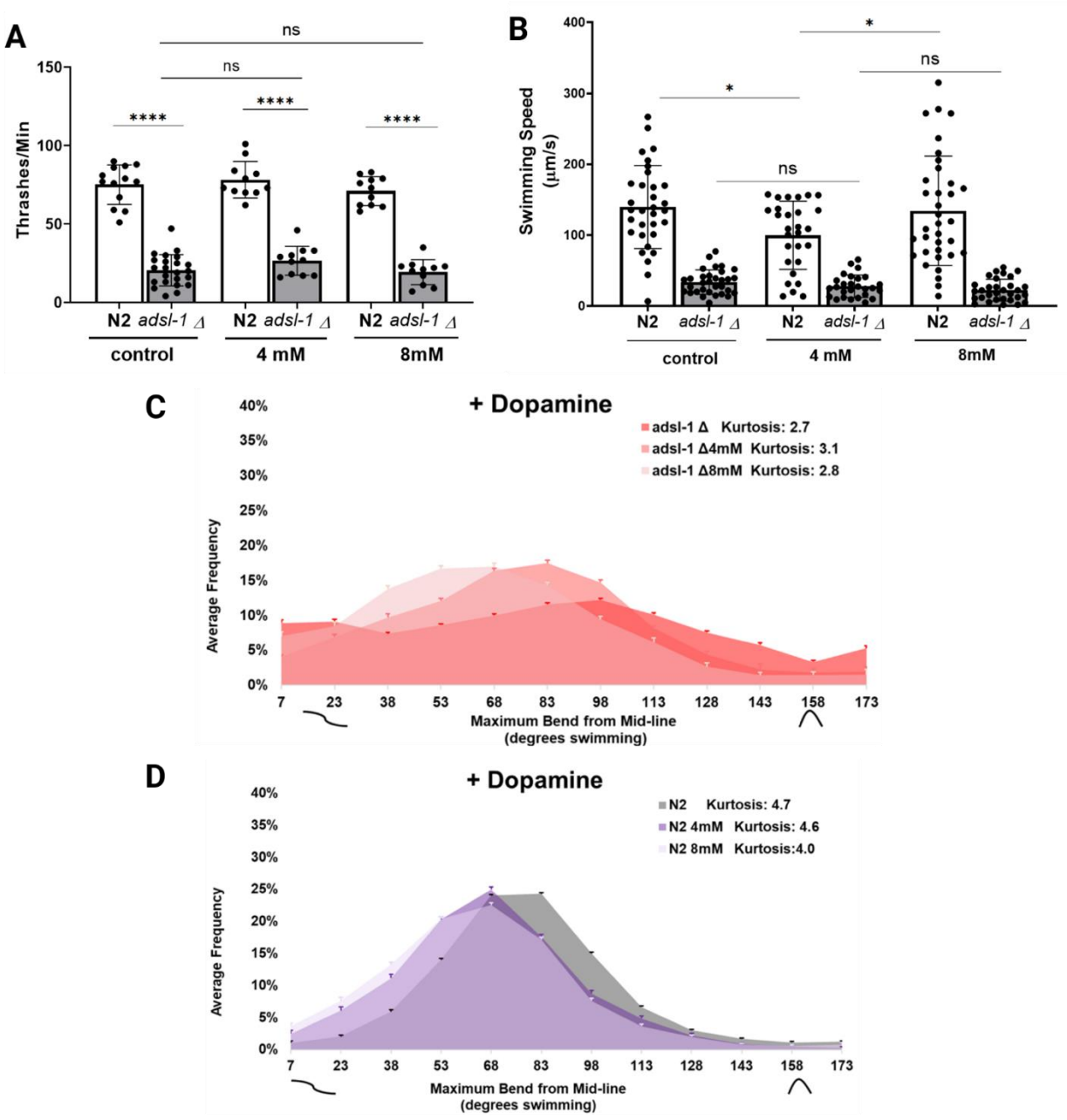

Figure 8. Exogenous dopamine may impair muscular function. Thrashing rates, swimming speeds, and maximum bending angle distribution of *adsl-1(tm3328)* mutants (A, B and C) and N2 animals (A, B, and D) supplemented with various concentrations of dopamine are compared. In panels A and B, each dot represents one animal, and an ordinary one-way ANOVA with Tukey's multiple comparisons test was performed to determine significance. * corresponds to $p<0.05$ and **** corresponds to $p<0.0001$. In panel C, *adsl-1* n = 73, *adsl-1 Δ* 4mM n = 27, and *adsl-1 Δ* 8mM n = 31. In panel B, *adsl-1 Δ* 4mM n = 27, *adsl-1 Δ* 8mM n = 31, and *adsl-1 Δ* measurements are taken from 32 of the *adsl-1 Δ* in panel C. In panels B and D, measurements are taken from the same 32 N2, 28 N2 4mM, and 35 N2 8mM animals. Measurements in panel A are derived from animals assayed in panel B.

Chapter 3

Investigating Alternative Hypotheses About Etiology of the *adsl-1* Coordination Phenotype.

My experiments exploring head oscillation behavior paired with the work of my lab has shown that *adsl-1* deficient *C. elegans* can be effective in modeling ADSL Deficiency-related neurobehavioral symptoms. Analyzing *adsl-1* deficient *C. elegans* neurobehavior is just one of the ways we can study the neurological symptoms associated with ADSL Deficiency, but patients suffer from devastating neuromuscular symptoms too. Although *adsl-1*-related muscle structure defects are involved in neuromuscular coordination, *adsl-1* function in the neuron likely plays a key role as well. We are interested in using the *adsl-1* coordination phenotype to study the role of neuronal *adsl-1* in neuromuscular coordination as opposed to the role of *adsl-1* function in the muscle.

In Chapter 2, I found evidence supporting the hypothesis that perturbations to tyrosine metabolism are unlikely to cause *adsl-1* mutants' inability to regulate the angles at which they bend their bodies during swimming movement. In addition to causing defects in tyrosine metabolism, an *adsl-1* deficiency has other pleiotropic effects on *C. elegans*. Animals with an *adsl-1* deficiency have perturbations to energy metabolism and muscle structural defects. To determine if these defects contribute to the animals' ability to regulate body bending, I assessed coordination of mutants with muscle structural defects and perturbations to energy metabolism.

Muscle Structure Defects Alone do not Cause the *adsl-1* Coordination Phenotype

Loss of *adsl-1* function disrupts muscle myosin organization and reduces muscle mass[23]. Nahabedian *et al*. 2012 found that animals with muscle structural defects and reduced mobility also lacked the ability to generate normal sized bending amplitudes[30]. Two mutants from this study, *unc-82* and *unc-95*, produce smaller bending amplitudes. This phenotype is likely due to muscle structural defects that hinder muscle function[30]. *unc-82* encodes a set of polypeptides with a protein kinase domain near its N-terminus. Mutants with knockout of *unc*-82 are slow and have defects in localization of components of M-line and thick filaments[32]. *unc-95* encodes a protein that localizes to the M-lines, dense bodies, and muscle cell nuclei and has a LIM domain at its C-terminus. Knockout of *unc-95* results in slow or paralyzed movement and disorganized sarcomere structure [33,34].

I hypothesized that muscle structure defects, which hinder generation of normal bending amplitudes, may also lead to a lack of bending angle coordination. To determine if muscle structural defects contribute to the bending angle phenotype of *adsl-1* mutants, I analyzed the swimming behavior of *unc-82(e1323)* and *unc-95(ok893)* mutants.

As expected, *unc-82* animals swam (Figure 9B) and thrashed (Figure 9A) significantly slower than the N2 control. Their mean maximum bend angle was 11% smaller than control ($p = 0.057$), and the distribution of those angles was left-skewed with a peak between 60° and 90° compared to the normal distribution of N2 animals (Figure 9E). *unc-95* animals had significantly reduced swimming speeds (Figure 9D) and thrashing rates (Figure 9C) as well. Their mean maximum bend angle was 19% smaller than control ($p = 0.012$), and their bend angle distribution was left-skewed with a peak between 60° and 90° (Figure 9F). Left skewing and reduced mean maximum bending angle agrees with the bending amplitude phenotypes observed by Nahabedian *et al*. 2012 and reflects the animals swimming with smaller bend angles due to muscle weakness.

Although *unc-82* and *unc-95* mutants are weak and swim with smaller bends, both bend angle distributions contain distinct peaks suggesting that these animals maintain the ability to regulate the angles at which they bend restricting it to a window of smaller sized bending intensities during a bout of swimming. These results further support the hypothesis that muscle weakness underlies mobility defects observed upon the loss of *adsl-1* function. On the other hand, muscle structure defects alone are insufficient to recreate the bend angle phenotype associated with an *adsl-1* deficiency. I conclude that *adsl-1*-related loss of muscle integrity alone is unlikely to cause animals to lose the ability to regulate body bend angles.

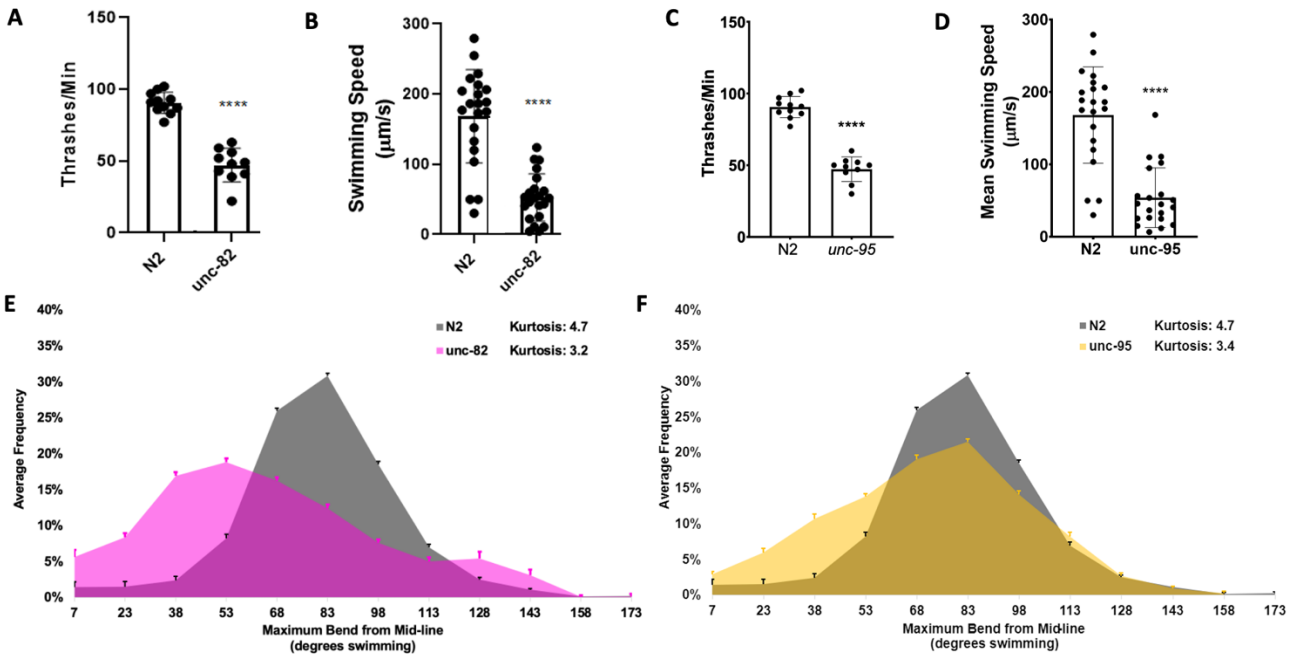

Figure 9. Muscle structure defects slow mobility and reduce the size of swimming bend angles. Thrashing and swimming speeds of *unc-82(e1323)* mutants (A and B) and *unc-95*(ok893) mutants (C and D) support the role of muscle integrity in *adsl-1* mobility. An ordinary one-way ANOVA with Tukey's multiple comparisons test was used to determine significance in panels A-D. **** corresponds to $p<0.0001$. Bending angle distributions (E and F) are skewed left suggesting that *unc-82(e1323)* and *unc-95(ok893)* swim with smaller bending angles. In panels B and E, measurements are taken from the same 21 N2 animals and 22 *unc-82(e1323)* animals. Measurements in panel A are derived from animals assayed in B and E. In panels D and F, measurements are taken from the same 21 N2 animals and 21 *unc-95(ok893)* animals. Measurements in panel C are derived from animals assayed in panels D and F.

General Unhealthiness does not Lead to Coordination Phenotypes

Because the loss of *adsl-1* activity has such a strong effect on the overall health of *adsl-1* animals, I hypothesized that general unhealthiness may cause the coordination phenotype. To determine if this was the case, I observed the swimming movement of other animals that share a generally unhealthy nature. Unhealthiness, in this scenario, is defined as having perturbations to energy metabolism and slowed development.

The mitochondrial complex I mutant strain *nuo-6(qm200)* has slowed embryonic and post-embryonic development as well as low oxygen consumption, reduced brood size, increased embryonic and larval lethality, extended lifespan, slowed swimming, and slowed pumping[35]. The nicotinamidase mutant strain *pnc-1(pk9605)* has egg-laying and gonadal development defects[36] as well as reduced NAD^+ production[37].

To determine if these mutants shared coordination phenotypes with *adsl-1* mutants, I compared their swimming behavior to that of the N2 control strain. I expected *nuo-6* animals would have slowed swimming speed as it has been previously reported that they have slowed rates of thrashing[35]. As expected, *nuo-6* animals thrashed (Figure 10C) and swam (Figure 10D) significantly slower than the N2 control. The angles at which they bent were tightly regulated (Figure 10F). *pnc-1* mutants swam (Figure 10B) and thrashed (Figure 10A) significantly slower than the N2 control. In their bending angle distribution, there was presence of a peak that was shifted towards the right in comparison to N2 (Figure 10E). This suggests that *pnc-1* animals retain the ability to regulate bending angle with preference for slightly larger bends than N2.

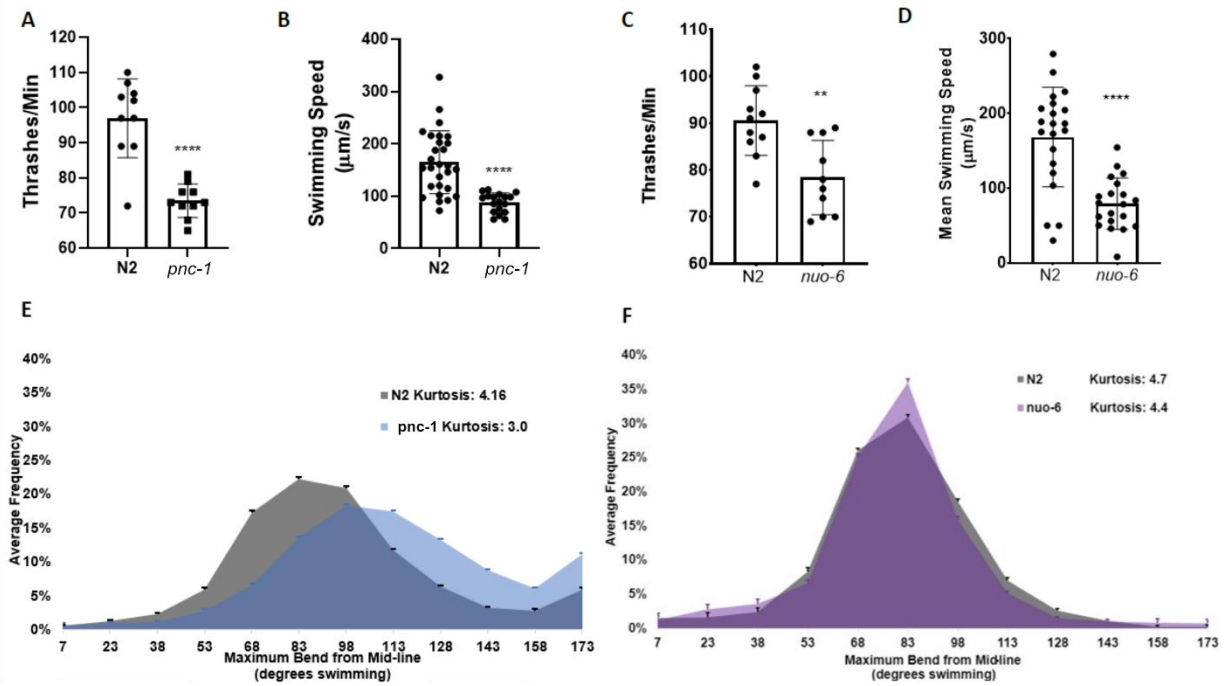

Figure 10. Mutants with perturbations to energy metabolism are slow but remain coordinated. Thrashing and swimming speeds of *pnc-1(pk9605)* mutants (A and B) and *nuo-6(qm200)* mutants (C and D) support that the pleiotropic effects of an *adsl-1* deficiency reduce mobility. A student's t test was used to determine significance in panels A-D. ** corresponds to $p<0.01$ and **** corresponds to $p<0.0001$. Bending angle distribution of *pnc-1(pk9605)* mutants (E) are shifted right and *nuo-6(qm200)* bending angle distribution (F) is tightly regulated. In panels B and E, measurements are taken from the same 28 N2 animals and 23 *pnc-1(pk9605)* animals. Measurements in panel A are derived from animals in panels B and E. In panels D and F, measurements are taken from the same 21 N2 animals and 20 *nuo-6(qm200)* animals. Measurements in panel C are derived from animals assayed in panels D and F.

I hypothesized that the right shift in bends may reflect higher instances of curling behavior. Upon observation of curling behavior, *pnc-1* mutants had significant increases in the percent time spent curling (Figure 11). I also observed curling behavior of *adsl-1* mutants and found that they too had increased percent time spent curling (Figure 11).

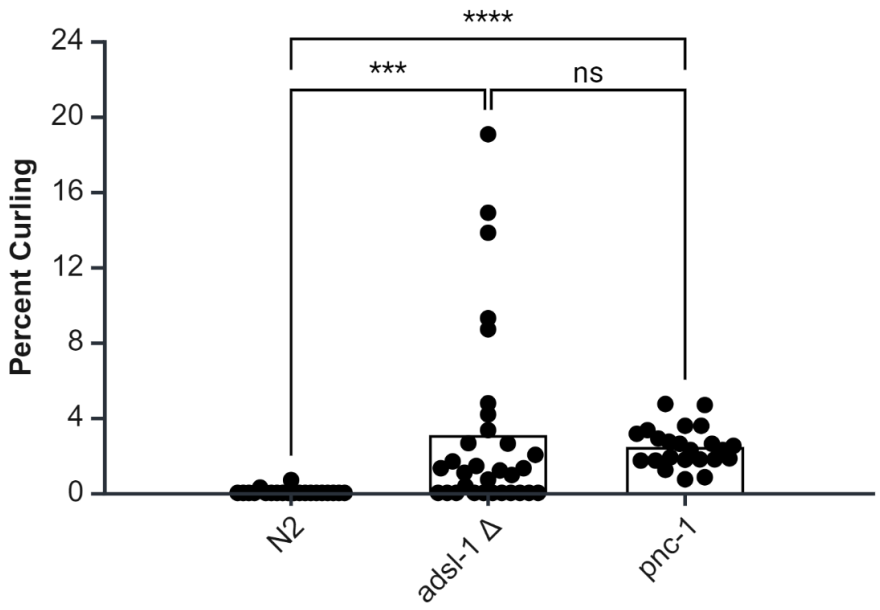

Figure 11. *pnc-1* and *adsl-1* mutants share phenotypes of increased percent curling. *adsl-1(tm3328)* (n = 31) and *pnc-1(pk9605)* (n = 23) mutants curl significantly more than N2 (n = 21). A Kruskal-Wallis test with Dunn's multiple comparisons test was performed to compare variance in mean percent curling. Each dot represents one animal. Boxes represent the interquartile range, bars represent upper and lower fences, and dots outside represent potential outliers. *** corresponds to $p<0.001$ and **** corresponds to $p<0.0001$.

Reduced rates of swimming and thrashing support that changes in energy metabolism might result in general unhealthiness which can contribute to mobility. However, the similarity of *nuo-6*, *pnc-1*, and N2 control animals bend angle distributions suggests that general unhealthiness alone does not contribute to regulation of bending angle. Based on these findings, I conclude that the lack of coordination during swimming movement is unlikely to be influenced by developmental defects and reduced energy metabolism associated with loss of *adsl-1* function.

Inability to Maintain Normal Rates of Locomotion is Not Sufficient to Induce Coordination Phenotypes

The coordination phenotype does not seem to correlate with muscle structural defects nor general unhealthiness. Further, a worm can be significantly slower than N2 control animals but remain highly coordinated. To take a broader approach in determining the mechanisms that underlie coordination, I sought to determine if inability to maintain normal rates of locomotion directly causes the coordination defect. To complement experiments exploring the effects of slow locomotion, I observed swimming behavior of the *ok2703* mutant strain which carries a deletion in *spp-1* and *umps-1* and has hyperactive muscle contractions as described by a significant increase in thrashing rate[38]. *spp-1* encodes a protein that is part of the SaPosin like protein family and enables channel activity by contributing to the formation of the pore complex during defense response to other organisms[39,40]. The *umps-1* gene encodes the uridine monophosphate synthetase protein which functions in pyrimidine biosynthesis as both orotate phosphoribosyltransferase and orotate monophosphate decarboxylase[41].

To determine if hyperactive muscle activity, or increased rate of thrashing, had any effect on coordination, I observed locomotion of *ok2703* animals. As expected, this mutant thrashed at significantly higher thrashing rates (Figure 12A) and swam with significantly higher speeds (Figure 12B) in comparison to the N2 control. Coordination did not change (Figure 12C). These data suggest that hyperactive muscle contractions do not cause animals to lose their ability to regulate body bend angles during swimming movement. These results, paired with the results from previous experiments in this chapter, suggest that changes in the animals' ability to maintain normal rates of locomotion are not sufficient to induce the coordination defect. Independently, I conclude that deletion of the portions of *spp-1* and *umps-1* as described by the *ok2703* strain do not directly cause animals to lose the ability to regulate body bending, which had never been examined before.

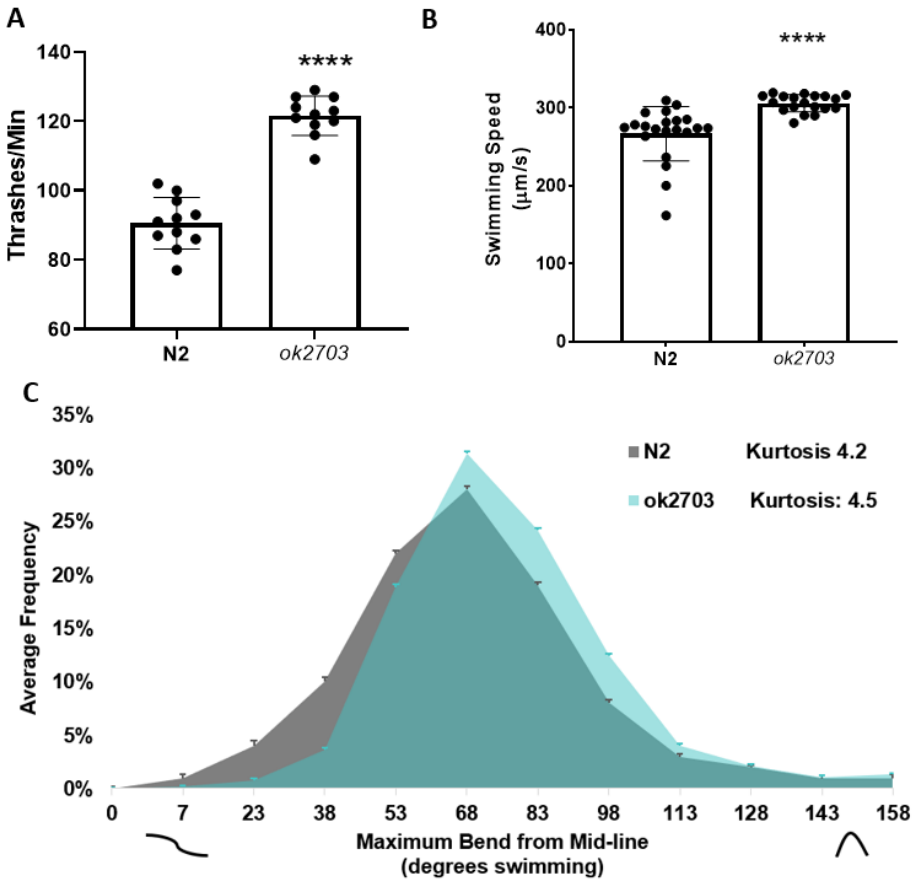

Figure 12. *ok2703* mutants are fast but remain coordinated. Thrashing and swimming speeds of *ok2703* mutants (A and B) provide evidence that agrees with the previously observed hyperactive muscle phenotype. A student's t test was used to determine significance in panels A. A Mann-Whitney test was used to determine significance in panel B. **** corresponds to $p<0.0001$. Bending angle distribution of *ok2703* mutants (C) suggests that the animals maintain the ability to tightly regulate body bending. In panels B and C, measurements are taken from the same 19 N2 animals and 21 *ok2703* animals. Measurements in panel A are derived from animals in panels B and C.

Chapter 4

Discussion

Throughout this thesis, I sought to determine the mechanisms that underlie the defects in neuromuscular coordination that arise upon the loss of *adsl-1* activity. My work demonstrating that *adsl-1* mutants phenocopy head oscillation behavior of *tdc-1* mutants contributed to our conclusion that reduced *adsl-1* activity results in the loss of tyramine signaling.

Currently, there is no mechanism known to connect tyrosine metabolism and purine biosynthesis, and whether loss of tyramine occurs via effects at the gene level or the protein level is unclear. It has been hypothesized that SAICAR/SAICAr toxicity may inhibit *tdc-1* expression or protein function as treatments to prevent production of SAICAR rescue *tdc-1* dependent phenotypes[18]. Evidence supporting SAICAR toxicity as a cause of some *adsl-1*-related phenotypes has also been found when treatments to reduce SAICAR production rescued thrashing behavior[21]. Because these treatments, often LMX or MTX, help to restore thrashing behavior, it would be beneficial to determine if this same approach can be used to rescue neuromuscular coordination.

Tyrosine is synthesized in 4 cell types: RIC interneurons, RIM motor neurons, gonadal sheath cells, and UVI cells[24]. Previously, tyramine was thought to only serve as a precursor for octopamine in these cells. However, it has been found to act as a neurotransmitter in the RIM neurons and UV1 cells[24]. As head oscillation behavior is a complex coordination event hypothesized to be controlled by a neural circuit involving sensory neurons, command neurons, interneurons, and motor neurons[42,43], I reasoned that perturbations to these signaling events via loss of tyramine production may also cause the coordination defects associated with the loss of *adsl-1* function. My results suggest that perturbations to this system, through loss of tyramine production, had no effect on locomotion.

Tyrosine accumulation in *adsl-1* deficient animals is curious as only 4 cell types are known to produce tyramine[24]. Due to this small number of tyramine-producing cells, I reasoned that tyrosine

accumulation could be a result of general perturbations to tyrosine metabolism and that perhaps dopamine production is also affected upon the loss of *adsl-1* activity. Analysis of dopamine deficient mutants and dopamine supplementation suggest that if general perturbations to tyrosine metabolism exist, they are not likely to contribute to the locomotive phenotypes associated with the loss of *adsl-1* activity. Instead, exogenous dopamine caused animals to swim with smaller sized bending angles. It is possible that as dopamine concentrations increase, the animals may be subject to partial swimming induced paralysis. Swimming induced paralysis occurs when dopamine cannot be cleared from the synapse at rates quick enough to prevent extra synaptic activity[25]. This would result in animals moving with smaller sized bending angles as they lack the ability to properly contract and relax their muscles to create a normal bend. If excess dopamine induces smaller sized bending angles, this may describe the left-skew of maximum body bend angles observed upon dopamine supplementation (Figure 8C, Figure 8D).

By observing coordination of animals that have muscular structural defects like *adsl-1* mutants, I found evidence further supporting previous hypotheses that muscular structural defects contribute to *adsl-1* animal's slowed mobility[23]. These muscle mutants maintain the ability to regulate the angles at which they bend. However, they lack the strength required to produce normal sized bends[30]. Similarly, animals with general unhealthiness are slow, yet maintain their ability to coordinate locomotion. Unlike *nuo-6* animals, *pnc-1* mutants body bend angle distribution is slightly shifted towards larger bending angles. This shift is likely a result of the curling phenotype that arises upon the loss of *pnc-1* function. The cause of this increase in curling behavior remains unclear.

Curling events have been found to progressively increase with age[44]. One hypothesis that may explain the increase in *pnc-1* percent curling is due to the loss of nicotinamidase function which results in decreased levels of nicotinic acid (NA) and nicotinamide (NAD^+)[37]. NAD^+ levels are known to decrease in aged worms[45]. Loss of nicotinamidase function could induce age-related phenotypes if NAD^+ concentrations are decreased. This curling phenotype provides an explanation for bending angles that appear on the right side of Figure 10E around 180°, but the cause of increased curling remains unclear as

the animals assayed are just Day 1 old adults. If perturbations to NAD^+ metabolism induce age-related phenotypes, perhaps *adsl-1* animals also have reduced NAD^+. Using metabolomics, we could determine whether NAD^+ levels are altered upon the loss of *adsl-1* function.

Muscle mutants and animals with perturbations to energy metabolism were slow. *ok2703* mutants were fast. All strains maintained the ability to coordinate body bending. This suggests that changes in mobility, specifically an overall increase or decrease in the speed of locomotion or the rate of thrashing, are not connected to changes in coordination.

My findings suggest that the development of phenotypes that occur upon the loss of *adsl-1* function are not controlled by a single mechanism. Instead, altered learning is likely due to perturbations to tyramine signaling[18] and slowed mobility may be due to muscle weakness, perturbations to energy metabolism, or SAICAR/SAICAr toxicity[21]. How the coordination phenotype arises remains less clear as this phenotype does not seem to be controlled by the same mechanisms that underlie the phenotypes of altered learning or slowed mobility.

I hypothesize that the coordination phenotype develops largely due to *adsl-1* function in the neurons that are involved in mechanosensory-mediated proprioception. During movement, *C. elegans* sense and respond to the medium they are in or upon in order to move towards food or from noxious substances. A variety of mechanosensory neurons are involved in these processes. These neurons transduce signals to the interneurons which further send signals to the motor neurons. Motor neurons are a key component of the neuromuscular junction which is essential in generating the action potential required for muscle contraction and body bending.

Among its presence in various cell types, *adsl-1* is expressed in ventral and dorsal D-type motor neurons, ventral B-type motor neurons, inner labial 2 sensory neurons, dorsorectal ganglion ventral process motor/interneurons (Table 1)[46]. These neurons play a role in proprioception or coordination of dorsal-ventral body wall muscle contraction. It is possible that reduced *adsl-1* expression in these cell types could cause the lack of coordination upon the loss of *adsl-1* activity through perturbations to

proprioception or mechanosensation. Future experiments designed to study movement of N2 animals with cell-specific reduction of *adsl-1* function or *adsl-1* animals with cell-specific restoration of *adsl-1* function in these neurons may reveal a role for *adsl-1* in neuromuscular coordination.

Table 1. CeNGEN Report of *adsl-1* expression in neuronal cell types.

Gene Name				*adsl-1* (WBGene00011064)			
threshold				2			
Cell Type	**Expression**	**Cell Type**	**Expression**	**Cell Type**	**Expression**	**Cell Type**	**Expression**
I6	129.05	**AVL**	21.43	**AQR**	12.74	**NSM**	5.43
PVP	128.30	**CAN**	21.30	**RMF**	12.00	**AIA**	5.18
I2	92.53	**ASG**	21.20	**PVR**	11.87	**BDU**	4.97
LUA	83.26	**MC**	21.04	**FLP**	11.81	**RMH**	4.91
VD_DD*	60.23	**SMB**	20.73	**AIZ**	11.65	**ASJ**	4.76
SIA	53.73	**RME_DV**	20.22	**RIC**	11.38	**AIY**	4.44
RIF	48.58	**PHC**	19.42	**RMD_LR**	10.11	**ADL**	4.42
IL2_DV*	44.60	**AVD**	18.36	**DVC**	9.76	**PDE**	4.42
VB02*	40.90	**PDB**	17.61	**AVK**	9.65	**ASK**	4.41
AVA	38.77	**AS**	17.53	**RIV**	9.63	**AVF**	4.39
SIB	35.27	**ASEL**	17.33	**CEP**	9.51	**AWC_OFF**	4.28
RIB	32.96	**DB***	17.33	**AWA**	9.44	**AIB**	4.24
VB*	31.58	**VC**	16.86	**AFD**	9.36	**M1**	4.00
RIP	31.13	**AVJ**	16.75	**ASH**	9.29	**RIS**	3.98
PQR	29.05	**SMD**	16.37	**AVB**	8.96	**PVQ**	3.75
RMD_DV*	26.47	**AVG**	16.37	**ADF**	8.57	**BAG**	3.75
DVB*	26.32	**ALA**	16.02	**RMG**	8.38	**URX**	2.67
PHB	25.52	**VA**	15.86	**SAB**	8.32	**ASER**	0.42
URY	25.52	**DA**	15.45	**IL2_LR**	8.31		
RIR	25.40	**ASI**	15.39	**PVT**	8.02		
PLN	25.39	**HSN**	14.89	**AVE**	7.94		
RIA	25.36	**MI**	14.54	**AWC_ON**	7.16		
RIM	24.81	**I5**	14.28	**M2**	7.16		
AIN	24.55	**RID**	13.75	**PVW**	7.06		
DB01*	24.50	**AVM**	13.65	**ALM**	6.24		
VB01*	23.60	**ADA**	13.04	**AIM**	6.16		
SDQ	23.41	**PVM**	13.02	**I1**	6.10		
M5	23.39	**PHA**	12.98	**PVC**	5.97		
AUA	22.41	**PLM**	12.97	**RIG**	5.96		
URA	21.95	**AWB**	12.80	**AVH**	5.73		

*Cell types in red highlight neurons involved in mechanosensory-mediated proprioception or coordination of dorsal-ventral body wall muscle contraction.

Because *adsl-1* is expressed in neurons that are important for locomotion, and *adsl-1*-related coordination phenotypes are not a result of perturbations to tyramine signaling, irregular muscle structure, general unhealthiness, or an animal's inability to maintain normal rates of locomotion, the coordination phenotype could be an effective model for understanding the neuromuscular phenotypes associated with ADSL Deficiency. This phenotype is likely due to a more complex mechanism that could involve a combination of *adsl-1* related defects. Understanding if coordination phenotypes are due to neuronal function of *adsl-1* will expand our understanding of why ADSL Deficiency is accompanied by such severe neurological and neuromuscular symptoms. Further, this research may lead us to discovering new targets for therapeutic strategies that aim to alleviate ADSL-related neuromuscular symptoms.

Chapter 5

Methods

C. elegans culture and strains

Strains were maintained on OP50 *Escherichia coli* under standard conditions at 20°C[47]. The N2, MT13113 *tdc-1(n3419),* CB1112 *cat-2(e1112),* VC672 *unc-95(ok893),* MQ1333 *nuo-6(qm200),* CB1323 *unc-82(e1323),* and RB2045*(ok2703)* were obtained from the Caenorhabditis Genetics Center. HV727 *pnc-1(pk9605)* is a null allele[48] and HV854 *adsl-1(tm3328/hT2)* is an outcrossed strain. The allele is homozygous sterile and is balanced with hT2 that causes pharyngeal expression of GFP. Non-GFP homozygous *adsl-1(tm3328)* animals were picked for phenotypic analysis. For all experiments, gravid adults were placed onto a fresh NGM plate, allowed to lay eggs for 6 hours and then removed. Animals were synchronized by picking animals in the L4-stage and aging them for 24 hours. All experiments were conducted on Day 1 old adults.

Head Oscillation Assay

Day 1 adults were transferred onto an empty NGM plate and allowed to acclimate for one minute. After one minute had passed, the animal was stroked along its body as described in [24] and scored according to whether they oscillated their head during the induced reversal.

Supplementation Experiments

Stock solutions were prepared and filter-sterilized then added to OP50-seeded NGM plates to indicated final concentrations. After addition of the stock, plates were incubated at room temperature for 1-2 days prior to use. Tyramine hydrochloride (Millipore Sigma): 667 mM stock solution in water, used at 10mM plate concentration. Dopamine hydrochloride (Sigma-Aldrich): 266.6 mM stock solution in water, used at 4 mM and 533 mM stock solution in water, used at 8 mM plate concentration.

Locomotive Analysis

Thrashing rates were obtained by counting the number of thrashes committed during one minute of swimming. Parameters listed in Table 2 were collected using WormLab® software. Gravid adults were placed on normal or supplemented OP50 seeded NGM plates, allowed to lay eggs for 6 hours, then removed. One the animals developed into mid-L4 hermaphrodites, they were transferred to normal or supplemented OP50 seeded NGM plates and aged one day prior to the assays. After one day, 5-15 animals were placed on unspotted NGM plates in 50uL of M9 solution and allowed to acclimate at room temperature for 1 minute. After 1 minute of acclimation, 1-minute videos were recorded. A Nikon lens attached to a Basler acA2440 Camera at video mode 2456x2052 Mono 8 setting was used. 14 or 30 frames per second were collected on a light background.

Analysis of videos was performed by setting the threshold to a point where the software could differentiate between the worms and the background. 3-4 animals were used by the software to determine baseline body measurements and identify individual worm tracks for each frame[49].

Table 2. WormLab® Parameters

Parameter	Definition	Data Preparation
Crawling Speed	Distance per second covered by the worm along its central axis. Negative speeds represent backwards movement.	The absolute value of all speeds was averaged for each animal. Speeds above 500 um/sec were censored as they are typically associated with the loss and re-establishment of an animal while it is being tracked.
Swimming Speed	Traveling swimming speed of an animal measured over a two-stroke interval. Negative speeds represent backwards movement.	The absolute value of all speeds was averaged for each animal. Speeds above 500 um/sec were censored as they are typically associated with the loss and reestablishment of an animal while it is being tracked
Bending Angle	Maximum bending angles that were extracted from "Bend angle mid-point" dataset in which angles are measured between the midpoint-head and midpoint-tail segments of the animal.	R code (below) determined extracted maximum bend angle by determining if the angle before or after is less than or greater than the angle at hand. If less, then the angle at hand counted as a maximum bend.
Percent Curling	The relative percentage that an animal spends bent around so far that it overlaps with itself.	N/A
Mean Width	Width of dorsal-ventral cross-section animal averaged over the entire length of the animal.	N/A
Straight-line Distance	Shortest distance between centroids at the beginning and end of a worm track.	N/A
Distance Traveled in Reverse	Total distance traveled in reverse.	N/A
Cumulative Reversal Time	Total time the worm spends traveling in reverse.	N/A
Attenuation	How well the depth of a wave is maintained as it propagates along the body.	N/A

Maximum bending angles were extracted from Bend Angle Mid-Point statistics using the following code written in R Studio:

```
samplename<-read.csv(file.choose())
library(plyr)
library(reshape2)
library(zoo)
names <- colnames(samplename)
peak<-c()
output <- c(1:2000)
a <- Sys.time()
for(j in 1:length(names))
{ for(i in 2:1799){
    if(!is.na(samplename[i-1,j])&!is.na(samplename[i,j])&!is.na(samplename[i+1,j])){
      if(samplename[i,j]>samplename[i-1,j]&samplename[i,j]>samplename[i+1,j]){
        peak<-rbind(peak,c(samplename[i,j]))}}}
  output <- cbind(output,as.vector(unlist(peak)))
  peak <- c()}
b <- Sys.time()
a-b
output <- output[,-1]
Column1<-output[,1]
Column2<-output[,2]
Column3<-output[,3]
Column4<-output[,4]
Column5<-output[,5]
```

```
Column6<-output[,6]
Column7<-output[,7]
Column8<-output[,8]
newColumn1<-unique(Column1)
newColumn2<-unique(Column2)
newColumn3<-unique(Column3)
newColumn4<-unique(Column4)
newColumn5<-unique(Column5)
newColumn6<-unique(Column6)
newColumn7<-unique(Column7)
newColumn8<-unique(Column8)
n <- max(length(newColumn1), length(newColumn2),
length(newColumn3),length(newColumn4), length(newColumn5), length(newColumn6),
length(newColumn7), length(newColumn8))
length(newColumn1)<-n
length(newColumn2)<-n
length(newColumn3)<-n
length(newColumn4)<-n
length(newColumn5)<-n
length(newColumn6)<-n
length(newColumn7)<-n
length(newColumn8)<-n
CombinedData<-cbind(newColumn1,newColumn2,newColumn3,newColumn4,
                    newColumn5,newColumn6,newColumn7,newColumn8)
print(CombinedData)
```

```
write.table(CombinedData,file = "samplename.csv",sep = ",",row.names=FALSE,na='')
```

Statistical Analysis

Statistical analysis was performed using GraphPad Prism or BioRender Graph. Test details are described in each figure legend and provided in Appendix B.

RNAi

The *hprt-1* RNAi clone was from the *C. elegans* RNAi Library (Source BioScience, Nottingham, UK). Gravid adults were transferred to seeded RNAi plates, allowed to lay eggs for 6 hours, then removed. Those animals were allowed to develop to the L4 stage. Mid-L4 hermaphrodites were transferred to a new seeded RNAi plate and aged one day. Day-1 old adults were used for analysis. The *E. coli* strain HT115 carrying the empty RNAi vector L4440 was used as a control.

Appendix A

Modeling Lesch-Nyhan Syndrome in *C. elegans*

Lesch-Nyhan Syndrome

Lesch-Nyhan Syndrome is a rare X-linked inborn error of purine metabolism caused by a deficiency in the activity of the purine salvage enzyme HGPRT. It was first characterized by William Nyhan and Michael Lesch who described severe neurological defects and self-injurious behavior in a pair of brothers[50].

HGPRT recycles hypoxanthine to IMP and guanine to GMP (Figure 2). Patients with LNS experience severe neurological and muscular defects including intellectual disability, muscle ataxia, and self-injurious behavior[50]. As a result of upregulated *de novo* purine synthesis by the cell in response to failed purine salvage, uric acid levels in the blood of patients with LNS are elevated[50]. Assays measuring HGPRT activity in erythrocytes are the standard method for diagnosing LNS[51]. There is a spectrum of HGPRT deficiencies as a variety of mutations in the HGPRT gene exist. This spectrum includes patients with complete loss of HGPRT activity, who are diagnosed with the classical "Lesch-Nyhan variant", and patients with partial loss of HGPRT activity. Patients with partial function are diagnosed with either the "neurological variant" if they experience neurological defects or the "partial variant" if they suffer from hyperuricemia alone[52].

High levels of uric acid have been hypothesized to cause the neurological defects associated with LNS. Reduction of uric acid via treatment with allopurinol, a xanthine oxidoreductase inhibitor commonly used to treat gout, reduces accumulation of uric acid but does not impede the development of neurological symptoms[53]. Other methods used to reduce the severity of hyperuricemia include limiting purine consumption and increasing fluid intake.

There are no current strategies for treating the neurological behaviors associated with LNS. Low levels of serotonin in mice lead to an increase in aggressive behavior[54]. These findings lead others to hypothesize that self-injurious behaviors could be due to a lack of serotonin in the brain of patients with LNS. Treatments promoting serotonin production suppressed self-injurious behavior temporarily, but these results could not be replicated in later experiments[55,56].

Positron emission tomography uncovered perturbations to neuronal dopamine neurotransmission as a result of reduced dopamine decarboxylase activity[57]. Treatments promoting the production of dopamine had variable effects on neurological symptoms and of the positive effects, none were as effective as serotonin[58].

Erythrocytes of patients with LNS have increased levels of AICAR, AICAr, S-AMP, NA, NAD^+, and UDGP and reduced levels of ATP and GTP[59–61]. Their fibroblasts also have increased levels of AICAR and decreased levels of ATP, but only when they are grown in a medium with physiological levels of folate, rather than in the standard high-folate medium[62]. These cell models are useful for investigating metabolic and cellular changes associated with the loss of HGPRT function. However, there is a lack of animal models.

A mouse model with Hprt knockout in the brain results in accumulation of AICAR [63,64]. Rats that had dopaminergic signaling interrupted in early life model the self-injurious and aggressive behaviors associated with LNS when given levodopa, a dopamine precursor, in later life[65]. There are no current models that exhibit neurological or muscular defects due to reduced HGPRT activity.

Because there is a lack of animal models to study LNS, I sought to model it in *C. elegans*. To generate this model, I genetically manipulated the N2 *C. elegans* strain using RNAi targeting *hprt-1*, the *C. elegans* homolog of HGPRT. Using WormLab Imaging System, I determined if any neurological or muscular defects arise with reduced *hprt-1* function.

Duration of Backing Becomes Shorter upon Reduction of *hprt-1* Expression

I hypothesized that RNAi knockdown of *hprt-1* in *C. elegans* would result in phenotypic changes that could be used to study LNS. Upon RNAi knockdown, mean width, distance traveled in reverse, and cumulative reversal time were decreased, and straight-line distance and attenuation were increased (Table 3). Straight line distance is the shortest distance between the center of the worm's body at the beginning and the end of a recording[49]. Attenuation is a measure of how well the depth of a body wave is maintained during its propagation down an animal's body while swimming[49]. In this analysis, attenuation is reported as a percentage. 0% means that the wave depth was equal at the beginning and end of a body wave. The more positive an attenuation value is, the larger the difference between the wave depth at the beginning and the end of the wave. A negative attenuation value can occur due to backwards movement.

There were no changes in speed, the number of reversals, percent curling, or regulation of body bending angles (Figure 13). Further qRT-PCR analysis of *hprt-1* knockdown by our lab suggests that *hprt-1* expression is significantly reduced. These results suggest that *hprt-1* knockdown via RNAi results in a decrease in the duration of time spent backing, an increase in animal's ability to maintain body waves of a certain depth during swimming, an increase in how far an animal travels away from its starting point, and a decrease in the width of its body.

Table 3. Results from WormLab Analysis of *hprt-1* (RNAi) animals.

Parameter	Average		P-value
	EV	*hprt-1*	
Crawling Speed (um/s)	219.8	217.1	0.862
Mean Worm Length (um)	1030.7	1064.5	0.087
Mean Width (um)	81.5	75.5	0.004
Mean Area (um^2)	85394.6	81920.9	0.200
Straight-line Distance (um)	4669.6	6748.3	0.035
Wavelength (um)	562.4	578.7	0.314
Mean Amplitude (um)	68.3	64.0	0.313
Max Amplitude (um)	183.5	176.2	0.451
Turn Count	18.7	18.0	0.720
Distance Traveled Forward(um)	10525.0	11663.3	0.376
Distance Traveled in Reverse(um)	2992.3	884.0	0.004
Number of Reversals	2.7	1.4	0.054
Cumulative Reversal Time (s)	11.3	3.2	0.006
Cumulative Forward Time (s)	47.0	52.2	0.127
Number of Pirouettes	0.7	0.3	0.114
Pirouette Time (s)	1.3	0.6	0.111
Wave Initiation Rate	66.8	71.1	0.586
Body Wave Number	0.1	0.1	0.572
Attenuation	-14.6	12.5	0.044
Dynamic Amplitude (Stretch)	15.5	13.8	0.223
Asymmetry	0.0	0.0	0.693
Reverse Swim	0.2	0.1	0.193
Self-Contact Distance	0.4	0.3	0.700
Percent Curling	0.7	0.7	0.971
Brush Stroke	1.5	1.7	0.055
Activity	48.5	56.2	0.166
Swimming Speed (um/s)	144.20	150.48	0.782

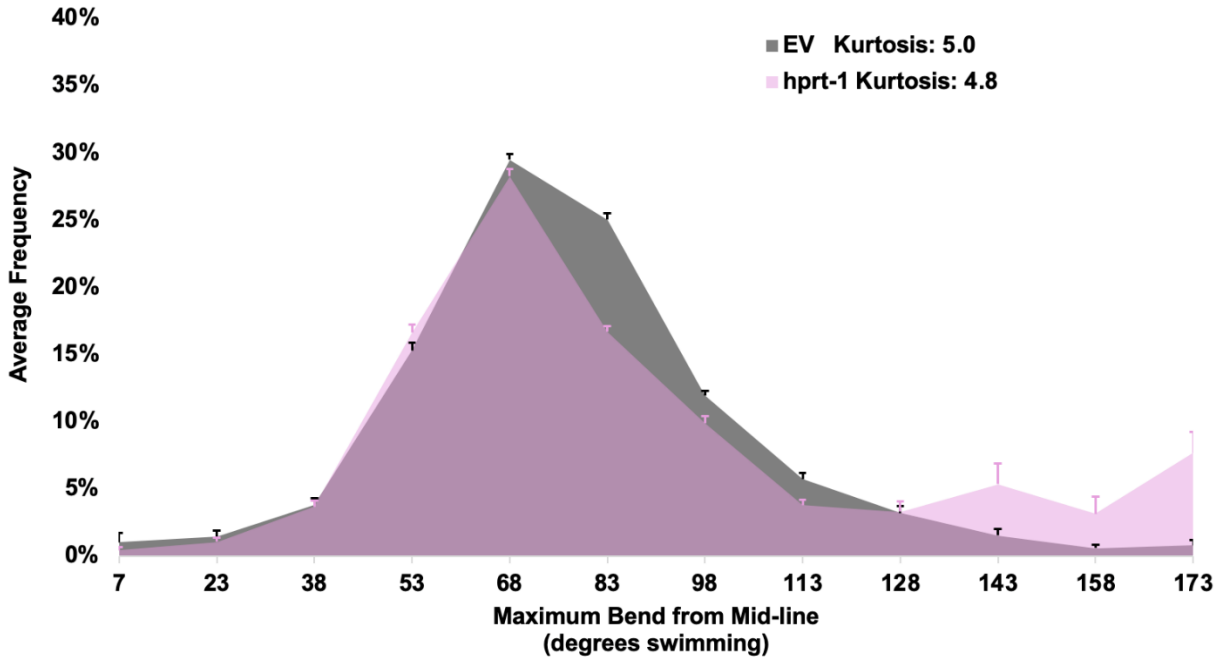

Figure 13. *hprt-1* (RNAi) animals are coordinated. Bending angle distribution of *hprt-1* (RNAi) animals suggests that the ability to regulate body bending during swimming movement is maintained. Bending angle distribution is from two replicates from two different *hprt-1* RNAi cultures. EV n = 20 and *hprt-1* n = 25.

Discussion

Through RNAi knockdown of *hprt-1* in *C. elegans*, I sought to create a model that could be used to study the mechanisms that underlie the neurological and muscular symptoms that are associated with LNS. My results paired with others from my lab suggest that *hprt-1* RNAi successfully reduces *hprt-1* expression in *C. elegans* which results in an increase in the distance an animal travels away from its starting point and an increase in the animal's ability to maintain a certain wave depth during its propagation down the body. *hprt-1* knockdown further reduces the duration of time spent backing and mean body width.

Although *hprt-1* knockdown causes phenotypic changes, I argue that these phenotypes are not useful for studying the neurological or muscular defects that arise due to reduced HGPRT activity in humans. Reduced body width could be due to a developmental defect. However, the difference in mean body width is only 6 um. This difference is significant. Yet, it is unlikely to be related to a developmental defect as mean body length and mean body area remain unchanged.

Attenuation is a phenotype that could be used to study neuromuscular coordination. However, in this analysis, the attenuation value for EV is negative. This negative value is likely due to backward swimming, and because the duration of backward swimming was increased, it is unlikely to be representative of EV animals' true ability to maintain a certain wave depth during the wave's propagation down the body. Analysis of attenuation should be standardized before it is used to study locomotion in future experiments.

The duration of time spent backing was higher for EV animals. This suggests that *hprt-1* animals do not travel as far or as long in reverse as control animals do. Typically, phenotypes that represent a neurological defect are an increase in the number of reversals or an increase in the time spent moving in reverse. If animals are reversing more frequently, they may have increased time spent in moving in reverse or the distance of backing, but EV and *hprt-1* animals had no change in the number of reversals.

Further, because *hprt-1* animals are not backing any more frequently or any longer than control animals, I argue that a decrease in the duration of reversal movement due to reduced *hprt-1* expression is not indicative of *hprt-1*-related neurological defects.

An increase in the straight-line distance, which is the distance between the center of the worm's body at the start and the end of a tracked recording[49], suggests that *hprt-1* animals travel further from their starting point in comparison to EV. Increased straight-line distance of *hprt-1* animals could be a result of EV animals traveling backward further or longer than *hprt-1* animals. This behavior could cause EV's overall displacement to be decreased if this backward movement is directed to the worm's starting point. Another explanation for increased straight-line distance of *hprt-1* animals is if they are turning less frequently than EV. An increase in turning may cause the worm's track to be more circular or to curve back toward its starting point which would reduce straight-line distance. Whether turning behavior has changed is unclear. Overall, straight-line distance is complex and alone is not useful to identify any neurological or muscular defects as several behavioral changes could influence its value.

hprt-1 animals have a slight preference for larger body bends as there is a slightly higher frequency of body bends between 143° and 173° in comparison to control animals. If *hprt-1* deficient animals mimic the metabolic changes associated with the loss of *hprt-1* function in erythrocytes, this increase could be a result of NAD^+ accumulation which could increase curling behavior. However, this shift is confusing as *hprt-1* animals do not curl any more than control and the metabolome of *hprt-1* deficient *C. elegans* has yet to be studied.

Why an *hprt*-1 deficiency in *C. elegans* fails to produce any neurological or muscular defects that would be useful for studying LNS is unclear. I hypothesize that there could be two scenarios that cause *hprt-1* deficient *C. elegans* to lack phenotypes useful for studying LNS. My first hypothesis is that RNAi knockdown only causes partial reduction of *hprt-1* and that any residual function is enough to prevent the onset of any neurological or muscular defects. This partial reduction would be similar to the LNS "partial variant". Studying the effects of *hprt-1* knockout in a mutant *C. elegans* strain would allow us to more

accurately model the classical "Lesch-Nyhan variant" with 0% HGPRT activity and determine if any neurological or muscular defects arise.

My second hypothesis is more complex. As mentioned before, fibroblasts of patients with LNS only exhibit metabolic changes when they are grown in mediums with physiological levels of folate. Folate cannot be synthesized *de* novo and the reduced form of folate, N^{10}-formyl-THF, is an important cofactor for the *de novo* purine synthesis enzymes GART and ATIC. If fibroblasts upregulate *de novo* synthesis in response to an HGPRT deficiency, N^{10}-formyl-THF will be used up much more quickly. Fibroblasts' metabolic changes only in response to reduced levels of folate suggest that an excess of folate in normal culture mediums provides a folate supply that is sufficient to sustain normal metabolite levels. In other words, cultures with physiological levels of folate have an insufficient folate supply that fails to allow upregulated *de novo* purine synthesis to proceed normally. Instead, folate may be depleted and GART and ATIC activity could be reduced. If ATIC activity is reduced, its substrate, AICAR, may accumulate.

Like humans, *C. elegans* rely on their diet to maintain folate supplies. One study revealed that *E. coli* used to feed *C. elegans* leads to folate accumulation in the gut. This accumulation reduces the animal's lifespan and treatments to reduce folate accumulation increases lifespan[66]. I hypothesize that folate may accumulate in the gut of *hprt-1* deficient animals providing a folate supply that is sufficient to prevent the onset of *hprt-1*-related phenotypes. I further hypothesize that if treatments are used to reduce folate accumulation in *C. elegans* through either exclusion of folate precursors in the nematode growth medium or inhibitor of *E. coli* folate production, neurological or muscular phenotypes that are more characteristic of LNS may arise.

Why would these phenotypes arise only when folate is reduced in *C. elegans*? The reaction catalyzed by *adsl-1* in *de novo* synthesis is reversible. Marsac *et al*. 2019 supplemented *C. elegans* with AICAR which resulted in accumulation of SAICAR, SAICAr, and AICAR[23]. If AICAR accumulates as a result of reduced ATIC activity, perhaps AICAR would be converted to SAICAR/r. SAICAR/r

accumulation could have toxic effects on various systems within the animals as it has been shown to negatively influence thrashing rates and learning[18,21]. Future experiments should explore phenotypes of mutant *C. elegans* with complete loss of *hprt-1* function and *hprt-1* animals with depleted folate levels.

Appendix B

Statistical Analysis

Table 4. Ordinary one-way ANOVA with Tukey's multiple comparisons test of *adsl-1(tm3328)* and *tdc-1(n3419)* percent suppression of head oscillations.

Alpha	0.05				
Tukey's multiple comparisons test	**Mean Diff.**	**95.00% CI of diff.**	**Significant?**	**Summary**	**Adjusted P Value**
N2 vs. *adsl-1* Δ	75.50	57.79 to 93.21	Yes	****	<0.0001
N2 vs. *tdc-1*	85.00	67.29 to 102.7	Yes	****	<0.0001
adsl-1 Δ vs. *tdc-1*	9.500	-8.210 to 27.21	Yes	****	<0.0001

Table 5. Unpaired t test of *tdc-1(n3419)* vs N2 Thrashing Behavior

N2 vs *tdc-1* Thrashing	
P value	0.0278
P value summary	*
Significantly different (P < 0.05)?	Yes
One- or two-tailed P value?	Two-tailed
t, df	t=2.394, df=18

Table 6. Unpaired t test of *tdc-1(n3419)* vs N2 Swimming Speed

N2 vs *tdc-1* Swimming Speed	
P value	0.0004
P value summary	***
Significantly different (P < 0.05)?	Yes
One- or two-tailed P value?	Two-tailed
t, df	t=3.928, df=36

Table 7. Unpaired t test of Effects of Tyramine (10mM) on Thrashing

***adsl-1 Δ* vs *adsl-1 Δ*+ Thrashing**	
P value	0.1737
P value summary	ns
Significantly different (P < 0.05)?	No
One- or two-tailed P value?	Two-tailed
t, df	t=1.390, df=33

Table 8. Unpaired t test of Effects of Tyramine (10mM) on Swimming Speed

***adsl-1 Δ* vs *adsl-1 Δ*+ Swimming Speed**	
P value	0.0426
P value summary	*
Significantly different (P < 0.05)?	Yes
One- or two-tailed P value?	Two-tailed
t, df	t=2.076, df=55

Table 9. Unpaired t test of *cat-2(e1112)* vs *adsl-1(tm3328)* Thrashing Behavior

***cat-2* vs *adsl-1* Thrashing**	
P value	<0.0001
P value summary	****
Significantly different (P < 0.05)?	Yes
One- or two-tailed P value?	Two-tailed
t, df	t=11.83, df=21

Table 10. Unpaired t test of *cat-2(e1112)* vs *adsl-1(tm3328)* Swimming Speed

***cat-2* vs *adsl-1* Swimming Speed**	
P value	<0.0001
P value summary	****
Significantly different (P < 0.05)?	Yes
One- or two-tailed P value?	Two-tailed
t, df	t=7.741, df=49

Table 11. Ordinary one-way ANOVA with Tukey's Multiple Comparisons Test of the Effect of Dopamine (4mM and 8mM) on *adsl-1(tm3328)* Thrashing Behavior

Alpha	0.05				
Tukey's multiple comparisons test	**Mean Diff.**	**95.00% CI of diff.**	**Significant?**	**Summary**	**Adjusted P Value**
N2 vs. *adsl-1 Δ*	54.64	44.21 to 65.07	Yes	****	<0.0001
N2 vs. N2 (4mM)	-3.105	-15.42 to 9.209	No	ns	0.9765
N2 vs. *adsl-1 Δ* (4mM)	48.53	36.22 to 60.85	Yes	****	<0.0001
N2 vs. N2 (8mM)	4.077	-8.237 to 16.39	No	ns	0.9264
N2 vs. *adsl-1 Δ* (8mM)	55.80	43.49 to 68.12	Yes	****	<0.0001
adsl-1 Δ vs. N2 (4mM)	-57.75	-68.77 to -46.73	Yes	****	<0.0001
adsl-1 Δ vs. *adsl-1 Δ* (4mM)	-6.111	-17.13 to 4.909	No	ns	0.5866
adsl-1 Δ vs. N2 (8mM)	-50.57	-61.58 to -39.55	Yes	****	<0.0001
adsl-1 Δ vs. *adsl-1 Δ* (8mM)	1.162	-9.857 to 12.18	No	ns	0.9996
N2 (4mM) vs. *adsl-1 Δ* (4mM)	51.64	38.82 to 64.45	Yes	****	<0.0001
N2 (4mM) vs. N2 (8mM)	7.182	-5.635 to 20.00	No	ns	0.5756
N2 (4mM) vs. *adsl-1 Δ* (8mM)	58.91	46.09 to 71.73	Yes	****	<0.0001
adsl-1 Δ (4mM) vs. N2 (8mM)	-44.45	-57.27 to -31.64	Yes	****	<0.0001
adsl-1 Δ (4mM) vs. *adsl-1 Δ* (8mM)	7.273	-5.544 to 20.09	No	ns	0.5621
N2 (8mM) vs. *adsl-1 Δ* (8mM)	51.73	38.91 to 64.54	Yes	****	<0.0001

Table 12. Ordinary one-way ANOVA with Tukey's Multiple Comparisons Test of the Effect of Dopamine (4mM and 8mM) on *adsl-1(tm3328)* Swimming Speed

Alpha	0.05				
Tukey's multiple comparisons test	**Mean Diff.**	**95.00% CI of diff.**	**Significant?**	**Summary**	**Adjusted P Value**
N2 vs. *adsl-1 Δ*	106.0	72.20 to 139.7	Yes	****	<0.0001
N2 vs. N2 (4mM)	39.86	4.919 to 74.80	Yes	*	0.0152
N2 vs. *adsl-1 Δ* (4mM)	111.7	76.44 to 147.0	Yes	****	<0.0001
N2 vs. N2 (8mM)	5.281	-27.75 to 38.31	No	ns	0.9974
N2 vs. *adsl-1 Δ* (8mM)	117.2	83.13 to 151.2	Yes	****	<0.0001
adsl-1 Δ vs. N2 (4mM)	-66.09	-101.0 to -31.15	Yes	****	<0.0001
adsl-1 Δ vs. *adsl-1 Δ* (4mM)	5.772	-29.51 to 41.06	No	ns	0.9971
adsl-1 Δ vs. N2 (8mM)	-100.7	-133.7 to -67.65	Yes	****	<0.0001
adsl-1 Δ vs. *adsl-1 Δ* (8mM)	11.20	-22.83 to 45.23	No	ns	0.9332
N2 (4mM) vs. *adsl-1 Δ* (4mM)	71.87	35.44 to 108.3	Yes	****	<0.0001
N2 (4mM) vs. N2 (8mM)	-34.58	-68.82 to -0.3436	Yes	*	0.0462
N2 (4mM) vs. *adsl-1 Δ* (8mM)	77.30	42.09 to 112.5	Yes	****	<0.0001
adsl-1 Δ (4mM) vs. N2 (8mM)	-106.4	-141.0 to -71.86	Yes	****	<0.0001
adsl-1 Δ (4mM) vs. *adsl-1 Δ* (8mM)	5.429	-30.12 to 40.98	No	ns	0.9979
N2 (8mM) vs. *adsl-1 Δ* (8mM)	111.9	78.57 to 145.2	Yes	****	<0.0001

Table 13. Ordinary one-way ANOVA with Tukey's Multiple Comparisons Test of *unc-82(e1323)* and *unc-95(ok893)* Thrashing Behavior

Alpha	0.05				
Tukey's multiple comparisons test	**Mean Diff.**	**95.00% CI of diff.**	**Significant?**	**Summary**	**Adjusted P Value**
N2 vs. *unc-82*	43.35	33.20 to 53.50	Yes	****	<0.0001
N2 vs. *unc-95*	43.35	33.20 to 53.50	Yes	****	<0.0001
unc-82 vs. *unc-95*	0.000	-10.39 to 10.39	No	ns	>0.9999

Table 14. Ordinary one-way ANOVA with Tukey's Multiple Comparisons Test of *unc-82(e1323)* and *unc-95(ok893)* Swimming Speed

Alpha	0.05				
Tukey's multiple comparisons test	**Mean Diff.**	**95.00% CI of diff.**	**Significant?**	**Summary**	**Adjusted P Value**
N2 vs. *unc-82*	115.5	79.64 to 151.5	Yes	****	<0.0001
N2 vs. *unc-95*	114.3	77.93 to 150.6	Yes	****	<0.0001
unc-82 vs. *unc-95*	-1.295	-37.20 to 34.61	No	ns	0.9959

Table 15. Unpaired t test of N2 vs *pnc-1(pk9605)* Thrashing Behavior

N2 vs *pnc-1(pk9605)* Thrashing	
P value	<0.0001
P value summary	****
Significantly different (P < 0.05)?	Yes
One- or two-tailed P value?	Two-tailed
t, df	t=6.094, df=18

Table 16. Unpaired t test of N2 vs *pnc-1(pk9605)* Swimming Speed

N2 vs *pnc-1(pk9605)* Swimming Speed	
P value	<0.0001
P value summary	****
Significantly different (P < 0.05)?	Yes
One- or two-tailed P value?	Two-tailed
t, df	t=5.293, df=44

Table 17. Unpaired t test of N2 vs *nuo-6(qm200)* Thrashing Behavior

N2 vs *nuo-6(qm200)* Thrashing	
P value	0.0018
P value summary	**
Significantly different (P < 0.05)?	Yes
One- or two-tailed P value?	Two-tailed
t, df	t=3.628, df=19

Table 18. Unpaired t test of N2 vs *nuo-6(qm200)* Swimming Speed

N2 vs *nuo-6(qm200)* Swimming Speed	
P value	<0.0001
P value summary	****
Significantly different (P < 0.05)?	Yes
One- or two-tailed P value?	Two-tailed
t, df	t=5.339, df=39

Table 19. Nonparametric one-way ANOVA with Dunn's Multiple Comparisons test of *adsl-1(tm3329)* and *pnc-1(pk9605)* Percent Curling

Alpha	0.05			
Dunn's multiple comparisons test	**Mean rank diff.**	**Significant?**	**Summary**	**Adjusted P Value**
N2 vs. *adsl-1 Δ*	-23.41	Yes	***	0.0003
N2 vs. *pnc-1*	-36.69	Yes	****	<0.0001
adsl-1 Δ vs. *pnc-1*	-13.28	No	ns	0.0664

Table 20. Students t test of *ok2703* Thrashing Behavior

***ok2703* Thrashing**	
P value	<0.0001
P value summary	****
Significantly different (P < 0.05)?	Yes
One- or two-tailed P value?	Two-tailed
t, df	t=11.01, df=20

Table 21. Mann Whitney test of *spp-1* & *ump-1(ok2703)* Swimming Speed.

***ok2703* Swimming Speed**	
P value	<0.0001
Exact or approximate P value?	Exact
P value summary	****
Significantly different (P < 0.05)?	Yes
One- or two-tailed P value?	Two-tailed
Sum of ranks in column A,B	258 , 562
Mann-Whitney U	27

BIBLIOGRAPHY

1. Jurecka, A. & Tylki-Szymanska, A. Inborn errors of purine and pyrimidine metabolism: a guide to diagnosis. *Mol Genet Metab* **136**, 164–176 (2022).
2. van Gennip, A. H., Bierau, J. & Nyhan, W. L. Inborn errors of purine and pyrimidine metabolism. in *Physician's Guide to the Treatment and Follow-Up of Metabolic Diseases* 245–253 (Springer Berlin Heidelberg, Berlin, Heidelberg, 2006). doi:10.1007/3-540-28962-3_25.
3. Wevers, R. A. *et al.* 1H-NMR Spectroscopy of body fluids: inborn errors of purine and pyrimidine metabolism. *Clinical chemistry* **45**, 539-548 (1999).
4. van Gennip, A. H. Defects in metabolism of purine and pyrimidines. *Nederlands Tijdschrift voor Klinische Chemie* **24**, 171–175 (1999).
5. Mitchell, G. & McInnes, R. R. Differential diagnosis of cerebral palsy: Lesch-Nyhan syndrome without self-mutilation. *Can Med Assoc J* **130**, 1323–1324 (1984).
6. Pedley, A. M. & Benkovic, S. J. A new view into the regulation of purine metabolism: the purinosome. *Trends in Biochemical Sciences* **42**, 141–154 (2017). doi:10.1016/j.tibs.2016.09.009.
7. Van Den Berghe, G., Bontemps, F., Vincent, M. F. & Van Den Bergh, F. The purine nucleotide cycle and its molecular defects. *Progress in Neurobiology* **3**, 547-561 (1992).
8. Kmoch, S. *et al.* Human adenylosuccinate lyase (ADSL), cloning and characterization of full-length cDNA and its isoform, gene structure and molecular basis for ADSL deficiency in six patients. *Human Molecular Genetics* **9**, 1501-1513 (2000).
9. Jaeken, J. & Van den Berghe, G. An infantile autistic syndrome characterised by the presence of succinylpurines in body fluids. *Lancet* **2**, 1058–1061 (1984).
10. Jurecka, A. *et al.* Clinical, biochemical and molecular findings in seven Polish patients with adenylosuccinate lyase deficiency. *Mol Genet Metab* **94**, 435–442 (2008).

11. Mouchegh, K. *et al.* Lethal fetal and early neonatal presentation of adenylosuccinate lyase deficiency: observation of 6 patients in 4 families. *Journal of Pediatrics* **150**, 57-61.e.2 (2007).

12. Donti, T. R. *et al.* Diagnosis of adenylosuccinate lyase deficiency by metabolomic profiling in plasma reveals a phenotypic spectrum. *Mol Genet Metab Rep* **8**, 61–66 (2016).

13. Salerno, C. *et al.* Effect of d-ribose on purine synthesis and neurological symptoms in a patient with adenylosuccinase deficiency. *Biochimica et Biophysica Acta (BBA) - Molecular Basis of Disease* **1453**, 135–140 (1999).

14. Jurecka, A., Tylki-Szymanska, A., Zikanova, M., Krijt, J. & Kmoch, S. D-ribose therapy in four Polish patients with adenylosuccinate lyase deficiency: absence of positive effect. *J Inherit Metab Dis* **31 Suppl 2**, S329-S332 (2008).

15. Salerno, C., Crifo, C., Curatolo, P. & Ciardo, F. Effect of uridine administration to a patient with adenylosuccinate lyase deficiency. *Advances in experimental medicine and biology* **486**, 75-78 (2000).

16. Van den Bergh, F., Vincent, M. F., Jaeken, J. & Van den Berghe, G. Functional studies in fibroblasts of adenylosuccinase-deficient children. *J Inherit Metab Dis* **16**, 425–434 (1993).

17. Dutto, I. *et al.* Pathway-specific effects of ADSL deficiency on neurodevelopment. *elife* **11**, e70518 (2022). doi:10.7554/eLife.70518.

18. Moro, C. A. *et al.* Adenylosuccinate lyase deficiency affects neurobehavior via perturbations to tyramine signaling in Caenorhabditis elegans. *PLoS Genet* **19**, e1010974 (2023). doi:10.1371/journal.pgen.1010974.

19. Jurecka, A., Zikanova, M., Kmoch, S. & Tylki-Szymańska, A. Adenylosuccinate lyase deficiency. *J Inherit Metab Dis* **38**, 231–42 (2015).

20. Stone, T. W. *et al.*Succinyl purines induce neuronal damage in the rat brain. In *Purine and Pyrimidine Metabolism in IX*. *Advances in experimental medicine and biology* **431**, 185-189 (1998).

21. Fenton, A. R. *et al.* A Caenorhabditis elegans model of adenylosuccinate lyase deficiency reveals neuromuscular and reproductive phenotypes of distinct etiology. *Mol Genet Metab* **140**, 107686 (2023).

22. Franklin, L. P. *et al.* The purine nucelotide cycle is important for coordination of muscle contractions during locomotion in C. elegans. (2024). [in revision]

23. Marsac, R. *et al.* Purine homeostasis is necessary for developmental timing, germline maintenance and muscle integrity in Caenorhabditis elegans. *Genetics* **211**, 1297–1313 (2019).

24. Alkema, M. J., Hunter-Ensor, M., Ringstad, N. & Horvitz, H. R. Tyramine functions independently of octopamine in the Caenorhabditis elegans nervous system. *Neuron* **46**, 247–260 (2005).

25. McDonald, P. W. *et al.* Vigorous motor activity in Caenorhabditis elegans requires efficient clearance of dopamine mediated by synaptic localization of the dopamine transporter DAT-1. *Journal of Neuroscience* **27**, 14216–14227 (2007).

26. Vidal-Gadea, A. *et al.* Caenorhabditis elegans selects distinct crawling and swimming gaits via dopamine and serotonin. *Proceedings of the National Academy of Sciences* **108**, 17504–17509 (2011).

27. Omura, D. T., Clark, D. A., Samuel, A. D. T. & Horvitz, H. R. Dopamine signaling is essential for precise rates of locomotion by C. elegans. *PLoS One* **7**, e38649 (2012). doi:10.1371/journal.pone.0038649.

28. Jiang, Y., Gaur, U., Cao, Z., Hou, S. T. & Zheng, W. Dopamine D1- and D2-like receptors oppositely regulate lifespan via a dietary restriction mechanism in Caenorhabditis elegans. *BMC Biol* **20**, (2022). doi: 10.1186/s12915-022-01272-9.

29. Gray, J. & Lissmann, H. W. The locomotion of nematodes. *Journal of Experimental Biology* **41**, 135–154 (1964).

30. Nahabedian, J. F., Qadota, H., Stirman, J. N., Lu, H. & Benian, G. M. Bending amplitude – a new quantitative assay of C. elegans locomotion: identification of phenotypes for mutants in genes encoding muscle focal adhesion components. *Methods* **56**, 95–102 (2012).

31. Karbowski, J. *et al.* Conservation rules, their breakdown, and optimality in Caenorhabditis sinusoidal locomotion. *J Theor Biol* **242**, 652–669 (2006).

32. Zengel, J. M. & Epstein, H. F. Identification of genetic elements associated with muscle structure in the nematode Caenorhabditis elegans. *Cell Motil* **1**, 73–97 (1980).

33. Hoppe, P. E., Chau, J., Flanagan, K. A., Reedy, A. R. & Schriefer, L. A. Caenorhabditis elegans unc-82 encodes a serine/threonine kinase important for myosin filament organization in muscle during growth. *Genetics* **184**, 79–90 (2010).

34. Broday, L. *et al.* The LIM domain protein UNC-95 is required for the assembly of muscle attachment structures and is regulated by the RING finger protein RNF-5 in C. elegans. *J Cell Biol* **165**, 857–867 (2004).

35. Yang, W. & Hekimi, S. Two modes of mitochondrial dysfunction lead independently to lifespan extension in Caenorhabditis elegans. *Aging Cell* **9**, 433–447 (2010).

36. Vrablik, T. L., Huang, L., Lange, S. E. & Hanna-Rose, W. Nicotinamidase modulation of NAD+ biosynthesis and nicotinamide levels separately affect reproductive development and cell survival in C. elegans. *Development* **136**, 3637–3646 (2009).

37. Wang, W. *et al.* Comparative metabolomic profiling reveals that dysregulated glycolysis stemming from lack of salvage NAD+ biosynthesis impairs reproductive development in Caenorhabditis elegans. *Journal of Biological Chemistry* **290**, 26163–26179 (2015).

38. Wang, Y. Determining the contributions of the spp-1 and umps-1 genes on the hyperactive muscle phenotype. (Schreyer Honors College, State College, 2018). [undergraduate thesis]

39. Hoeckendorf, A., Stanisak, M. & Leippe, M. The saposin-like protein SPP-12 is an antimicrobial polypeptide in the pharyngeal neurons of Caenorhabditis elegans and participates in defence against a natural bacterial pathogen. *Biochemical Journal* **445**, 205–212 (2012).

40. Bányai, L. & Patthy, L. Amoebapore homologs of Caenorhabditis elegans. *Biochimica et Biophysica Acta (BBA) - Protein Structure and Molecular Enzymology* **1429**, 259–264 (1998).

41. Merry, A., Qiao, M., Hasler, M. & Kuwabara, P. E. RAD-6: pyrimidine synthesis and radiation sensitivity in Caenorhabditis elegans. *Biochemical Journal* **458**, 343–353 (2014).

42. White, J. G., Southgate, E., Thomson, J. N. & Brenner, S. The structure of the nervous system of the nematode Caenorhabditis elegans. *Philosophical Transactions of the Royal Society of London. Series B, Biological Sciences* **314**, 1-340 (1986).

43. Chalfie, M. *et al.*The neural circuit for touch sensitivity in Caenorhabditis elegans. *The Journal of Neuroscience* **5**, 956-964 (1985).

44. Yao, V. *et al.* An integrative tissue-network approach to identify and test human disease genes. *Nat Biotechnol* **36**, 1091–1099 (2018).

45. Mouchiroud, L. *et al.* The NAD+/sirtuin pathway modulates longevity through activation of mitochondrial UPR and FOXO signaling. *Cell* **154**, 430–441 (2013).

46. Taylor, S. R. *et al.* Molecular topography of an entire nervous system. *Cell* **184**, 4329-4347.e23 (2021). doi:10.1016/j.cell.2021.06.023.

47. Brenner, S. The genetics of Caenorhabditis elegans. *Genetics* **77**, 71–94 (1974).

48. Vrablik, T. L., Huang, L., Lange, S. E. & Hanna-Rose, W. Nicotinamidase modulation of NAD+ biosynthesis and nicotinamide levels separately affect reproductive development and cell survival in C. elegans. *Development* **136**, 3637–3646 (2009).

49. Restif, C. *et al.* CeleST: computer vision software for quantitative analysis of C. elegans swim behavior reveals novel features of locomotion. *PLoS Comput Biol* **10**, e1003702 (2014). doi:10.1371/journal.pcbi.1003702

50. Lesch Michael & Nyhan William. A familial disorder of uric acid metabolism and central nervous system function. *American Journal of Medicine* **36,** 561–570 (1964).

51. Nyhan, W. L. Lesch-Nyhan Disease. *J Hist Neurosci* **14**, 1–10 (2005).

52. Bakay, B., Nissinen, E., Sweetman, L., Francke, U. & Nyhan, W. L. Utilization of purines by an HPRT variant in an intelligent, nonmutilative patient with features of the Lesch-Nyhan syndrome. *Pediatr Res* **13**, 1365–1370 (1979).

53. Jinnah, H. A. Lesch-Nyhan disease: from mechanism to model and back again. *Dis Model Mech* **2**, 116–21 (2009).

54. Giacalone, E., Tansella, M., Valzelli, L. & Garattini, S. Brain serotonin metabolism in isolated aggressive mice. *Biochem Pharmacol* **17**, 1315–1327 (1968).

55. Nyhan, W. L., Johnson, H. G., Kaufman, I. A. & Jones, K. L. Serotonergic approaches to the modification of behavior in the Lesch-Nyhan syndrome. *Appl Res Ment Retard* **1**, 25–40 (1980).

56. Nyhan, W. L. Dopamine function in Lesch-Nyhan disease. *Environ Health Perspect* **108 Suppl 3**, 409–11 (2000).

57. Ernst, M. *et al.* Presynaptic dopaminergic deficits in Lesch–Nyhan disease. *New England Journal of Medicine* **334**, 1568–1572 (1996).

58. Mizuno, T.-I. & Yugari, Y. Self-mutilation in Lesch-Nyhan syndrome. *The Lancet* **303**, 761 (1974).

59. Ceballos-Picot, I. *et al.* New biomarkers for early diagnosis of Lesch-Nyhan disease revealed by metabolic analysis on a large cohort of patients. *Orphanet J Rare Dis* **10**, 7 (2015).

60. Sidi, Y. & Mitchell, B. S. Z-nucleotide accumulation in erythrocytes from Lesch-Nyhan patients. *Journal of Clinical Investigation* **76**, 2416–2419 (1985).

61. Simmonds, H. A., Fairbanks, L. D., Morris, G. S., Webster, D. R. & Harley, E. H. Altered erythrocyte nucleotide patterns are characteristic of inherited disorders of purine or pyrimidine metabolism. *Clinica Chimica Acta* **171**, 197–210 (1988).

62. López, J. M. *et al.* Physiological levels of folic acid reveal purine alterations in Lesch-Nyhan disease. *Proceedings of the National Academy of Sciences* **117**, 12071–12079 (2020).

63. Tschirner, S. K. *et al.* Non-targeted metabolomics by high resolution mass spectrometry in HPRT knockout mice. *Life Sci* **156**, 68–73 (2016).

64. Kuehn, M. R., Bradley, A., Robertson, E. J. & Evans, M. J. A potential animal model for Lesch-Nyhan syndrome through introduction of HPRT mutations into mice. *Nature* **326**, 295–298 (1987).

65. Breese, G. R. *et al.* Neonatal-6-hydroxydopamine treatment: Model of susceptibility for self-mutilation in the Lesch-Nyhan syndrome. *Pharmacol Biochem Behav* **21**, 459–461 (1984).

66. Virk, B. *et al.* Excessive folate synthesis limits lifespan in the C. elegans: E. coli aging model. *BMC Biol* **10**, 67 (2012).

ACADEMIC VITA

Mia Peifer

EDUCATION

The Pennsylvania State University - Schreyer Honors College **University Park, PA**
B.S. in Biochemistry and Molecular Biology | Minor in Chemistry ***Class of 2024***
Honors in Biochemistry and Molecular Biology - Molecular and Cell Biology Option

EXPERIENCE

Undergraduate Researcher, Hanna-Rose Lab | The Pennsylvania State University **Jan 2022 – Present**

- Designed and conducted behavioral assays to develop new models for purine metabolic disorders,
- using the roundworm *C. elegans* as a model organism.
- Devised and carried out supplementation assays to elucidate the effects of various compounds
- on *C. elegans* movement and behavior.
- Managed and analyzed large data sets using Excel and R Studio to observe changes in *C. elegans* movement and behavior.
- Mentored incoming undergraduate students and trained lab members in using imaging technologies.
- Developed and composed various research proposals and poster presentations.

Learning Assistant | Advanced Cell and Molecular Biology, Eberly College of Science **Jan 2023 – May 2023**

- Advised a team of students investigating research areas including cell biology, genetics, and molecular biology using the model organism *C. elegans*.
- Mentored students in experimental design, laboratory techniques, data analysis, and data interpretation promoting their scientific growth and proficiency.

Learning Assistant | Organic Chemistry 1, Eberly College of Science **Aug 2022 – Dec 2022**

- Collaborated with the instructor to foster interactive learning environments.
- Conducted engaging 1-on-1 office hours to bridge the divide between experienced professors and beginner students.

PUBLICATIONS

- Moro C.A. *et al.* Adenylosuccinate lyase deficiency affects neurobehavior via perturbations to tyramine signaling in Caenorhabditis elegans. PLoS Genet **19(**9): e1010974. (2023) https://doi.org/10.1371/journal.pgen.1010974
- Franklin L.P. *et al*. The purine nucleotide cycle is important for coordination of muscle contractions during locomotion in C. elegans. (2024) [in revision]

PRESENTATIONS

The Allied Genetics Conference 2024 | Washington, D.C., *Poster* **March 2024**
Eberly College of Science: Undergraduate Poster Exhibition, *Poster* **October 2023**
24th International *C. elegans* Conference | Glasgow, Scotland, *Poster* **June 2023**
Penn State Undergraduate Exhibition, *Poster* **April 2023**
Eberly College of Science: Undergraduate Poster Exhibition, *Poster* **October 2022**
Penn State Undergraduate Exhibition, *Poster* **April 2022**

AWARDS

GSA Poster Award Honorable Mention, The Allied Genetics Conference Poster Session **March 2024**
Norman Freed Undergraduate Research Award, Eberly College of Science **October 2023**
2nd Place in Life Sciences, Eberly College of Science: Poster Exhibition **October 2023**
2023 | 2024 PRESTIGE Undergraduate Research Scholarship, Penn State CoEIB **August 2023**
Undergraduate Research Award, Eberly College of Science **November 2022**
1st Place in Health and Life Sciences, Penn State Undergraduate Exhibition **May 2022**
BMB Scholars Program, Penn State Eberly College of Science **March 2022**